Calcium transfer from the ER to other organelles for optimal signaling in *Toxoplasma gondii*.

Zhu-Hong Li[1], Beejan Asady[1,2], Le Chang[1], Miryam Andrea Hortua Triana[1], Catherine Li[1], Isabelle Coppens[2] and Silvia N.J. Moreno[1,3*]

[1]Center for Tropical and Emerging Global Diseases, Department of Computes Science, University of Georgia and [3]Department of Cellular Biology, University of Georgia, Athens, Georgia 30602

[2]Department of Molecular Microbiology and Immunology, Johns Hopkins Bloomberg School of Public Heath, Baltimore, MD 21205

Running title: Intracellular Ca^{2+} stores of *T. gondii*

[*]To whom correspondence should be addressed: Silvia N. J. Moreno, Department of Cellular Biology and Center for Tropical and Emerging Global Disease, 350A Paul D. Coverdell Center, University of Georgia, Athens, GA 30602. Tel.: 706-542-4736; Fax: 706-542-9493; E-mail: smoreno@uga.edu

Keywords: Calcium, endoplasmic reticulum, membrane contact sites, Toxoplasma gondii, SERCA-Ca^{2+}-ATPase, calcium tunneling

ABSTRACT

Ca^{2+} signaling in cells begins with the opening of Ca^{2+} channels in either the plasma membrane (PM) or the endoplasmic reticulum (ER) and results in a dramatic increase in the physiologically low (<100 nM) cytosolic Ca^{2+} level. The temporal and spatial Ca^{2+} levels are well regulated to enable precise and specific activation of critical biological processes. Ca^{2+} signaling regulates pathogenic features of apicomplexan parasites like *Toxoplasma gondii* which infects approximately one-third of the world's population. *T. gondii* relies on Ca^{2+} signals to stimulate traits of its infection cycle and several Ca^{2+} signaling elements play essential roles in its parasitic cycle. Active egress, an essential step for the infection cycle of *T. gondii* is preceded by a large increase in cytosolic Ca^{2+} most likely by release from intracellular stores. Intracellular parasites take up Ca^{2+} from the host cell during host Ca^{2+} signaling events to replenish intracellular stores. In this work, we investigated the mechanism by which intracellular stores are replenished with Ca^{2+} and demonstrated a central role for the SERCA-Ca^{2+}-ATPase in keeping not only the ER filled with Ca^{2+} but also other stores. We show mitochondrial Ca^{2+} uptake, by transfer of Ca^{2+} from the ER likely through membrane contact sites. We propose a central role for the ER in sequestering and redistributing calcium to other intracellular organelles following influx at the PM.

HIGHLIGHTS

- The *T. gondii* ER efficiently takes up Ca^{2+} that enters the cytosol from the extracellular milieu.
- Filling of acidic stores in *T. gondii* appears to be dependent on the filling of the ER
- The mitochondrion of *T. gondii* has no direct access to extracellular calcium but is able to take up Ca^{2+} by transfer from the ER and/or acidic stores

INTRODUCTION

Toxoplasma gondii is an intracellular parasite from the Apicomplexan Phylum that infects approximately one third of the world population (Weiss and Dubey, 2009). During the initial infection with *T. gondii*, the parasite engages in multiple rounds of a lytic cycle, which consists of invasion of host cells, replication inside a parasitophorous vacuole (PV), exit from the host cell causing its lysis followed by invasion of a new host cell (Black and Boothroyd, 2000; Blader *et al.*, 2015). Cytosolic Ca^{2+} ($[Ca^{2+}]_c$) fluctuations precede the activation of several key steps of the *T. gondii* lytic cycle like motility, attachment, invasion, and egress ($[Ca^{2+}]_c$) (Lourido and Moreno, 2015; Hortua Triana *et al.*, 2018). Egress from the host cell is an essential step for the infection cycle of *T. gondii* (Bisio and Soldati-Favre, 2019) and it was shown that it is preceded by a cytosolic Ca^{2+} increase (Endo *et al.*, 1982; Borges-Pereira *et al.*, 2015). Extracellular Ca^{2+} entry was demonstrated in extracellular (Pace *et al.*, 2014; Hortua Triana *et al.*, 2024) and intracellular replicating tachyzoites (Vella *et al.*, 2021). This activity was highly regulated and recent work from our lab showed that a TRP-like activity was involved (Marquez-Nogueras *et al.*, 2021).

Ca^{2+} signaling is part of the signaling pathways that regulate a large number of cellular functions (Clapham, 2007). All cells express a variety of channels, transporters, and Ca^{2+} pumps, located at the plasma membrane (PM) and/or intracellular organelles (endoplasmic reticulum (ER), acidic stores, and mitochondria) that regulate/control the concentration of cytosolic Ca^{2+} ($[Ca^{2+}]_c$). A high cytosolic Ca^{2+} concentration for sustained lengths of time, is toxic to cells and may result in their death (Bootman and Bultynck, 2020).

In *T. gondii*, both Ca^{2+} entry through the plasma membrane and influx from intracellular stores like the ER may initiate a cascade of signaling events important for the stimulation of the biological steps of the parasite lytic cycle (Lourido and Moreno, 2015; Hortua Triana *et al.*, 2018). Ca^{2+} oscillations were observed in motile parasites loaded with fluorescent Ca^{2+} indicators, (Lovett and Sibley, 2003) as well as expressing Genetically Encoded Calcium Indicators (GECIs) (Borges-Pereira *et al.*, 2015). The significance of Ca^{2+} signals during all stages of the lytic cycle has been demonstrated, but little is known about the mechanism by which intracellular stores contribute to cytosolic Ca^{2+} signals and downstream regulation.

The ER, an exclusive organellar feature of eukaryotic cells, is the main store for Ca^{2+} in most eukaryotic cells and it has been proposed that the ER is functionally heterogeneous with Ca^{2+} binding proteins and Ca^{2+} pumps and channels having a nonuniform distribution resulting in the presence of distinct subdomains within the organelle (Papp *et al.*, 2003). The ER in mammalian cells facilitates Ca^{2+} tunneling through its lumen as a mechanism of delivering Ca^{2+} to targeted sites without activating inappropriate processes in the cell cytosol (Petersen *et al.*, 2017). In addition, the ER is ubiquitously distributed and is in close contact with all cellular organelles and the plasma membrane (PM) (Spang, 2018). Over the past decade a new paradigm has emerged that seeks to decipher how subcellular organelles communicate with each other in order to coordinate activities and efficiently distribute ions and lipids within the cell. Numerous observations have highlighted the presence of tight, stable and yet non-fusogenic associations between organellar membranes which have since become known as membrane contact sites (MCSs) (Phillips and Voeltz, 2016).

The secretory pathway of *T. gondii* is organized in a highly polarized manner with the ER being an extension of the nuclear envelope (Hager *et al.*, 1999; Tomavo *et al.*, 2013). The ER at the apical surface of the nuclear envelope continues with the Golgi stacks and then the secretory organelles, micronemes and rhoptries, which are unique to the apicomplexan phylum (Hager *et al.*, 1999). These organelles perform important functions relevant to a successful lytic cycle like host cell attachment, invasion, and establishment of the parasitophorous vacuole (PV). Cytoplasmic Ca^{2+} increases, due to efflux from the ER, have been reported to initiate responses like microneme secretion (Carruthers and Sibley, 1999; Nagamune *et al.*, 2007b), conoid extrusion (Del Carmen *et al.*, 2009), invasion (Vieira and Moreno, 2000; Lovett and Sibley, 2003) and egress (Arrizabalaga and Boothroyd, 2004). These responses require precise spatiotemporal control of diverse targets and suggests the presence of distinct systems to deliver Ca^{2+} to specific locations rather than allowing global increases, which would activate unnecessary and potentially detrimental signaling events (Huet and Moreno, 2023).

In order to concentrate Ca^{2+} ions, the ER utilizes a SERCA-Ca^{2+}-ATPase, a transmembrane P-type ATPase, that couples ATP hydrolysis to the transport of ions across biological membranes and against a concentration gradient. SERCA pumps can be inhibited by various inhibitors including the very potent and highly specific thapsigargin (TG) (Thastrup *et al.*, 1990; Sagara and Inesi, 1991).

T. gondii expresses a SERCA Ca^{2+}-ATPase (TgSERCA), which possess SERCA conserved domains and Ca^{2+} binding sites and ATPase residues (Nagamune *et al.*, 2007a). The function of TgSERCA was determined by rescue experiments of yeast cells defective in Ca^{2+}-ATPases and by its specific inhibition by TG (Nagamune *et al.*, 2007a). TgSERCA was mainly localized to the ER of *T. gondii* but also showed a distinct distribution in extracellular parasites, where the protein was partially found in ER vesicles in the apical region near micronemes (Nagamune *et al.*, 2007a). This distribution pattern was different to the one obtained with the transient transfection of GFP-HDEL (an ER marker), which was retained near the nuclear envelope, suggesting an uneven distribution of ER markers in extracellular parasites. The authors suggested that this distribution to the apical end may be important for rapid release and effective recovery of cytosolic Ca^{2+}, events that likely govern both motility and microneme secretion (Nagamune *et al.*, 2007a; Nagamune *et al.*, 2007b).

In this work we characterize the mechanism by which the ER efficiently takes up Ca^{2+} promptly after the ion enters the cytosol from the extracellular milieu. We also characterized the role of the ER in transferring Ca^{2+} to other stores. We propose a model in which the ER is the distribution center for Ca^{2+} and due to the high Ca^{2+} affinity of the SERCA Ca^{2+}-ATPase the ER is highly efficient at storing Ca^{2+} and transferring it to other compartments.

RESULTS

The ER sequesters and redistributes Ca^{2+} to other organelles following PM influx

We first set up experiments to follow the destination of Ca^{2+} taken up by extracellular tachyzoites from the extracellular milieu into their cytosol. Tachyzoites were loaded with the ratiometric Ca^{2+} indicator Fura-2 and incubated in Ringer buffer containing 100 µM EGTA to chelate extracellular

106 Ca^{2+}, preventing its uptake, and investigated the release of intracellular Ca^{2+} pools by various
107 inhibitors.
108 When thapsigargin (TG), which inhibits the activity of SERCA, was added, it prevented the
109 re-uptake of Ca^{2+} into the ER and unmasked the leakage of Ca^{2+} from the ER into the cytosol,
110 causing a Ca^{2+} cytosolic increase of approximately 160 nM **(Fig. 1B and S1A)**. We compared this
111 with the effect of ionomycin (IO), a Ca^{2+}/H^{+} ionophore which acts on neutral intracellular Ca^{2+}
112 stores, inducing depletion of Ca^{2+}, mainly from the ER (Smith *et al.*, 1989). Exposure of *T. gondii*
113 to 1 μM ionomycin caused a cytosolic increase of approximately 700-1100 nM Ca^{2+} (**Fig. S1A-**
114 **B**). We next tested another SERCA inhibitor, cyclopiazonic acid (CPA), with a different mode of
115 action than TG. CPA caused a lower Ca^{2+} cytosolic increase than the one caused by TG, possibly
116 implying less specificity toward TgSERCA **(Fig. S1B).** Exposure of parasites to TG before CPA
117 ablated CPA's effect, but this did not occur when adding CPA prior to TG **(Fig. S1C-D)**. Although
118 TG does a better job at depleting the ER of Ca^{2+}, the increase of cytosolic Ca^{2+} after adding TG is
119 un-impressive compared to the effect of IO **(Fig. S1A)**. This result could indicate the presence of
120 other calcium stores not inhibited by TG or simply that TG was not very efficient at blocking
121 TgSERCA.
122 Next, we tested the effect of Ca^{2+} entry in the filling of intracellular stores by measuring the
123 cytosolic Ca^{2+} increases in response to inhibitors after pre-exposing the parasite suspension to
124 extracellular Ca^{2+} (**Fig. 1C-F,** *dark traces*). Addition of 1.8 mM Ca^{2+} caused a cytosolic increase
125 due to influx through a partially characterized plasma membrane pathway (**Fig. 1C**, *dark blue*
126 *trace*) (Pace *et al.*, 2014). This Ca^{2+} influx appeared to be immediately taken up by the ER as the
127 response to TG was much greater in parasites previously exposed to extracellular Ca^{2+} (compare
128 light and dark blue traces) (**Fig. 1C**). We next tested the lysosomotropic agent glycyl-L-
129 phenylalanine-naphthylamide (GPN), which mobilizes Ca^{2+} from acidic organelles (Haller *et al.*,
130 1996; Lloyd-Evans *et al.*, 2008; Miranda *et al.*, 2010; Yuan *et al.*, 2021) and observed a similar
131 pattern (**Fig. 1D**). The cytosolic Ca^{2+} increase upon addition of GPN in parasites previously
132 exposed to extracellular Ca^{2+} was much greater than in cells not exposed to extracellular Ca^{2+} (**Fig.**
133 **1D**, *compare light and dark blue traces*). A similar phenomenon was observed when adding
134 nigericin (acting on acidic stores) or CCCP (most likely acting on mitochondria) (**Figs 1E-F**, *dark*
135 *purple and orange traces, respectively*). These data indicated that the ER, mitochondrion, and the
136 Plant Like Vacuolar Compartment (PLVAC) and other acidic stores, all appear to have the ability
137 to take up Ca^{2+} following influx through the plasma membrane. The ER displayed high capacity
138 to access a large portion of extracellular Ca^{2+}, with TG producing close to ~500-700 nM of Ca^{2+}
139 increase after pre-exposure to Ca^{2+} and only ~150-200 nM Ca^{2+} without Ca^{2+} pre-exposure **(Fig.**
140 **1C)**.
141 In summary, upon pre-exposure of *T. gondii* to physiological levels of extracellular Ca^{2+}, the
142 ER, mitochondria, and acidic stores exhibited the capacity to release many times more Ca^{2+} than
143 without pre-exposure, with the ER and GPN-sensitive stores displaying the greatest response **(Fig**
144 **1G).**

145 We next hypothesized that if the ER is the most efficient organelle to access extracellular Ca^{2+}
146 and transfer it to the other organelles, it should be possible to see an increased response to agonists
147 like GPN or nigericin after inhibiting SERCA with TG permitting the buildup of Ca^{2+} on the
148 cytosolic side of the ER membrane. For the next experiment we added Ca^{2+} to fill the stores,
149 followed by TG to cause Ca^{2+} efflux from the ER, and then GPN (**Fig. 1H**). We compared the
150 response to GPN between plus and minus the addition of TG and observed that the cytosolic
151 increase caused by GPN when preceded by TG was significantly larger (**Fig. 1H**). We followed
152 the same approach with nigericin and observed that the response increased after the addition of
153 TG (**Fig. 1I**). These experiments support our hypothesis that extracellular Ca^{2+} can be used to fill
154 the ER and from the ER Ca^{2+} can be distributed to other organelles.
155
156 **Ca^{2+} uptake by the SERCA-Ca^{2+} ATPase in permeabilized tachyzoites**

157 The previous results highlighted an important role for the ER in taking up Ca^{2+} from the
158 cytoplasm after an increase due to influx from the extracellular milieu. We believe that this ER
159 uptake, essential for keeping stores filled with Ca^{2+}, is due to the high Ca^{2+} affinity of TgSERCA.
160 The SERCA functions as an essential mechanism for the ER to maintain its Ca^{2+} levels, an
161 especially important function considering the leakage of Ca^{2+} from the ER into the cytosol which
162 occurs constitutively and passively (Camello *et al.*, 2002).
163 We developed a protocol that allowed us to measure directly Ca^{2+} uptake by the store where
164 the SERCA is localized (ER), based on the compartmentation of a fluorescent dye in permeabilized
165 cells. We used the low affinity indicator MagFluo4 which has a Kd for Ca^{2+} of 22 μM (Rossi and
166 Taylor, 2020). The cytosolic concentration of Ca^{2+} in *T. gondii* is around ~70 nM (Moreno and
167 Zhong, 1996), which is considerably below the detection limit of MagFluo4. We loaded parasites
168 for an extended length of time and using high concentrations of MagFluo4-AM as the intention
169 was for the indicator to compartmentalize. At the end of the incubation, parasites were washed and
170 exposed to low concentration of digitonin, which permeabilized the plasma membrane leaving the
171 organellar membranes intact. Under these conditions we had parasites loaded with a Ca^{2+} indicator
172 inside organelles (**Fig. 2A**). We next determined the capacity of these permeabilized parasites to
173 take up Ca^{2+}. SERCA activity is dependent on the presence of Mg-ATP (**Fig. 2B**) and we added
174 this substrate under defined concentrations of Ca^{2+} (determined using the MaxChelator program).
175 (Bers *et al.*, 1994). We observed that under these conditions a consistent and reproducible Ca^{2+}
176 uptake was measured that was optimal at 220 nM Ca^{2+} and 500 μM MgATP (**Figs 2B-C**).
177 Validation that this activity was due to SERCA is shown in the experiment in which we added TG
178 highlighting the ER Ca^{2+} leakage (**Fig. 2D**). Note that the Ca^{2+} released by TG appears to be modest
179 but the Kd of the indicator is 22 μM so a small decrease is highly significant when considering the
180 amount of Ca^{2+} that it represents. IO at 1 μM was more effective at releasing Ca^{2+} as the minimum
181 reached is lower than the starting level of Ca^{2+}. This is because IO is acting on other compartments
182 in addition to the ER (**Fig. 2E**).
183 In summary, these results showed that we can measure the *T. gondii* tachyzoite TgSERCA
184 activity *in situ* in permeabilized parasites with the low affinity Ca^{2+} indicator MagFluo4. This

activity is dependent on MgATP and TG causes release of the accumulated Ca^{2+}. The larger effect of IO could be due to Ca^{2+} release from other compartments driven by other ATPases (TgA1).

TgSERCA and the *T. gondii* lytic cycle

To investigate the role of TgSERCA (TGGT1_230420) in the biology of *T. gondii* we created conditional KOs (*iΔTgserca*) by inserting a tetracycline regulatable element at the 5' end of the gene to control the expression of the gene with ATc (Sheiner *et al.*, 2011). In addition, we endogenously tagged TgSERCA with HA. We isolated clonal cell lines of *iΔTgserca* and clones expressing *iΔTgserca-HA* (**Fig. 3A**). Western blots (**Fig. 3B**) and immunofluorescence analysis (**Fig. S2**) showed that the expression of TgSERCA is tightly regulated by ATc and it is absent after 1.5 days in culture. The growth of the *iΔTgserca* was severely retarded when cultured in the presence of ATc as evaluated by plaque assays (**Fig. 3C-D**). In this assay, parasites engage in repetitive cycles of invasion, replication, and egress causing host cell lysis and formation of plaques in confluent monolayers infected with *T. gondii*. Replication was severely impacted after down regulation of SERCA, and parasites were unable to proceed after one or two replication cycles (**Fig 3E-F**). All (100%) PVs of the ATc cultured mutant contained 4 parasites or less (**Fig. 3F**, *bar graph on the right*). Invasion of host cells was also reduced in the *iΔTgserca* (+ATc) mutant (**Fig. 3G**) and egress stimulated by ionomycin, or natural egress followed pre-incubation with Compound 1, was significantly decreased. These results supported the relevance of the ER Ca^{2+} storage for natural or IO stimulated egress. Interestingly, when testing egress after the addition of saponin in the presence of extracellular Ca^{2+}, we observed that the tachyzoites egressed sooner (**Fig. 3H**, *saponin egress*). This could result by a faster cytosolic Ca^{2+} threshold reached because of the deficient activity of SERCA after saponin permeabilization and exposure to extracellular calcium combined with the natural efflux from the ER.

Ca^{2+} uptake by the SERCA-ATPase is essential for filling acidic Ca^{2+} stores

The *iΔTgserca* mutant showed a reduced response to TG (**Fig. 4A**), when measuring cytosolic calcium (**Fig. 4A**) which was also the case when adding TG after extracellular calcium to fill the store (**Fig. 4B**). This was most likely the result of reduced Ca^{2+} accumulation by the ER of the *iΔTgserca* (+ATc) mutant. Note that the change in Ca^{2+} in Fig. 4A (*TatiΔku80* cells) is larger than in Fig. 1B (RH strain) and we believe that the difference is related to the characteristics of each cell line (RH vs *TatiΔku80*). In addition, Mg-ATP-driven Ca^{2+} uptake by permeabilized cells measured with MagFluo4 showed no TgSERCA activity after 48 h of culture with ATc (**Fig. 4C**). This experiment validated the MagFluo4 approach for determination of SERCA activity. At 24 hours after culturing the parasites with ATc there was still some SERCA activity (Fig. 4C). Ca^{2+} entry measured in Fura2 loaded *iΔTgserca* (±ATc) parasites was not affected by the downregulation of TgSERCA (**Fig. 4D**). Interestingly, the cytosolic resting Ca^{2+} concentration was not affected in the *iΔTgserca* (+ATc) mutant (Fig. 4 A,B, D-H) pointing to a critical role of the plasma membrane Ca^{2+} pump in the homeostasis of cytosolic Ca^{2+}. The response to Zaprinast

224 was diminished but was still present (**Fig 4E**) indicating that Zaprinast acts by releasing Ca^{2+} from
225 the ER and from an additional compartment. Adding Zaprinast after calcium also resulted in a
226 reduced response in the mutant pre-incubated with ATc (**Fig 1F**). We next tested GPN, which acts
227 mostly on acidic stores and the response was also decreased (**Fig. 4G**). Adding GPN after
228 replenishing the cells with Ca^{2+} resulted in an increased response as we showed in Fig. 1, but this
229 response was also reduced when the mutant was grown with ATc (**Fig. 1H**). These results support
230 a link between the stores on which GPN is acting upon and the ER. Considering that
231 downregulation of SERCA impacted the ER storage of Ca^{2+} but did not affect cytosolic Ca^{2+}
232 uptake, the diminished response to GPN, indicates that the Ca^{2+} released/leaked from the ER plays
233 an important role in filling the GPN's targeted store.
234

235 **The mitochondrion takes up Ca^{2+} from the ER**

236 In mammalian cells, the high concentration of Ca^{2+} in the ER is important for the production of
237 mitochondrial ATP (Wenzel *et al.*, 2022). This is because of the close proximity between the ER
238 and mitochondria which allows for the directional flow of Ca^{2+} from the ER to the mitochondria
239 (Gincel *et al.*, 2001; Rapizzi *et al.*, 2002). With the aim of determining if the *T. gondii*
240 mitochondria can take up calcium, we introduced a genetic Ca^{2+} indicator in the mitochondrion of
241 *T. gondii* tachyzoites by attaching the *GCaMP6* gene (Chen *et al.*, 2013) to the mitochondrial
242 targeting signal of the *T. gondii* superoxide dismutase 2 (SOD2) gene (Pino *et al.*, 2007) and
243 isolated parasite clones (*Tgsod2gcamp6*) (Vella *et al.*, 2020). GCaMP6 was localized to the
244 mitochondria as detected by fluorescence (**Fig 5A**). Direct Ca^{2+} uptake was observed in digitonin
245 permeabilized parasites incubated in the presence of increasing concentrations of Ca^{2+} (**Fig 5B-C**).
246 A measurable increase was observed but high concentrations of Ca^{2+} were needed (**Fig. 5B-C**)
247 indicating that the *T. gondii* mitochondria can take up Ca^{2+} but with very low affinity and that the
248 concentrations of Ca^{2+} needed for the uptake were much higher than the concentrations of cytosolic
249 Ca^{2+} that are present in the cytosol of a healthy cell (**Fig 5B**).
250 We reasoned that the *T. gondii* mitochondrion could be taking up Ca^{2+} through close membrane
251 contacts with the ER as it is possible that the concentration of Ca^{2+} in those microdomains could
252 reach much higher levels than in the cytosol and would allow for mitochondrial uptake (Scorrano
253 *et al.*, 2019). We next loaded the *Tgsod2gcamp6* mutant with Fura2 and measured, first, if adding
254 extracellular Ca^{2+} to the parasite suspension led to an increase in GCaMP6 fluorescence. Parallel
255 experiments looking at cytosolic and mitochondrial Ca^{2+} showed that adding extracellular Ca^{2+}
256 does cause an increase in the cytosol, however mitochondrial Ca^{2+} was not affected (**Fig. 5D-E**).
257 We next added TG followed by Ca^{2+} and this led to an increase in cytosolic Ca^{2+} but only TG
258 resulted in a measurable increase in fluorescence of the mitochondrial indicator (**Fig 5G**). Our
259 interpretation is that after adding TG, there was accumulation of Ca^{2+} at the cytosolic side of the
260 ER membrane leading to an increased concentration of the ion which activated mitochondrial
261 uptake.
262 We next inserted the *SOD2GCaMP6* chimeric gene in the *iΔTgserca* mutant and isolated the
263 clonal mutant *iΔTgserca-sod2gcamp6.* We first looked at mitochondrial uptake after adding TG

264 and as shown previously, the parasites cultured without ATc showed a measurable and consistent
265 increase in GCaMP fluorescence after adding TG (**Fig. 5H**, *blue trace*). This was abolished in cells
266 cultured in the presence of ATc as the low expression of TgSERCA would result in ER depletion
267 of Ca^{2+} (**Fig. 5H,** *pink trace*). Interestingly, we observed an increase in the GCaMP fluorescence
268 after adding GPN, ionomycin or Zaprinast (**Fig. 5H-J,** *blue traces*). In all cases the fluorescence
269 increase was reduced in the *iΔTgserca* (+ATc) and the difference in the response was always
270 significant (**Fig. 5H-J,** *pink traces*).
271 In summary, we demonstrated that the mitochondrion of *T. gondii* can take up Ca^{2+} through
272 transfer from the ER, a phenomenon that becomes evident after blocking the ER uptake with TG
273 as the concentration of Ca^{2+} needed to activate the uptake is very high and only reachable at
274 membrane contact sites between the ER and mitochondria. The *iΔTgserca* (+ATc) mutant, is
275 unable to keep the ER filled with Ca^{2+} and this impacts the capacity of the mitochondria to take up
276 Ca^{2+}. The mitochondria could apparently take up Ca^{2+} directly from acidic stores, which became
277 depleted when TgSERCA was downregulated.
278
279 **Interaction between the ER and the mitochondrion and acidic compartments.**
280 We next investigated if it was possible to see interaction between the ER with other organelles by
281 IFA and/or EM. We performed IFAs with ER and mitochondria markers and ER and PLVAC
282 markers (**Fig. 6**). We observed that in intracellular parasites the mitochondrion surrounds the ER
283 and multiple potential points of interaction are seen (**Fig. 6A** and supplemental video 1). The
284 mitochondrion of intracellular *T. gondii* tachyzoites surrounds the periphery of the cell in a lasso-
285 shape morphology. In extracellular parasites the mitochondrion changes drastically its shape
286 adopting either a sperm-like or a collapsed conformation (Ovciarikova *et al.*, 2017) (**Fig. 6B** and
287 supplemental video 2). Our hypothesis is that this retraction of the mitochondrion allows the ER
288 to expand in extracellular parasites into ER tubules, which extend toward the apical domain of the
289 parasite where Ca^{2+} is needed for secretion of micronemes and conoid extrusion.
290 The PLVAC also showed points of contact with the ER (**Fig. 6C** and supplemental video 3).
291 Multiple points of contact were also observed by EM between the ER and the PLVAC, the ER and
292 the apicoplast and the ER and the mitochondrion (**Fig. 6D**).
293 Interestingly these contacts were still present in the *iΔTgserca* (+ATc) mutant (**Fig. S3, A-D**),
294 as most likely TgSERCA would not be directly involved in the establishment of contacts. We
295 quantified the length of the limiting membrane of the organelle in contact with ER tubules at a
296 distance of less than 30 nM and found that after knockdown of TgSERCA, the contact was not
297 altered. However, Calcium transported from the ER into the mitochondrion after thapsigargin
298 treatment was significantly decreased which means that this phenotype is due to reduced ER
299 Calcium and not to lack of contacts (**Fig. S3E**). A similar result was seen when measuring contacts
300 between the ER and the apicoplast (**Fig. S3F**) and between the ER and the PLVAC (**Fig. S3G**).
301 In summary, this data showed that the ER form contacts with other organelles like the
302 mitochondrion, the PLVAC and the apicoplast and these contacts could be the ones allowing the
303 transfer of Calcium from the ER, the store with the highest amount of Calcium, to the other

organelles. The SERCA high affinity for Calcium is critical for the filling of the ER. However, the molecular mechanisms involved in the uptake by the other organelles is less clear. Very little is known about the structure and composition of Membrane Contact Sites in *T. gondii* (Huet and Moreno, 2023). However, functional evidence for the transfer of Calcium has been demonstrated for the ER-apicoplast (Li *et al.*, 2021) and in this work we presented evidence for the transfer of Calcium between the ER and the mitochondrion and the ER and the PLVAC.

DISCUSSION

In this work we showed that the endoplasmic reticulum (ER) of *T. gondii* has an impressive capacity for capturing Ca^{2+} that enters the cytosol from the extracellular milieu, and it accomplishes this with a minimal increase in cytosolic Ca^{2+} levels. This is the result of a highly efficient SERCA Ca^{2+}-ATPase (TgSERCA) which also showed high affinity for Ca^{2+}. The TgSERCA activity combined with the plasma membrane Ca^{2+} pump (Luo *et al.*, 2001; Luo *et al.*, 2005) would not allow the cytosolic Ca^{2+} to increase above 200 nM (Hortua Triana *et al.*, 2024).

We also provide evidence of the ER's capacity for sharing Ca^{2+} with other organelles, which originates from the ER unique ability to capture a sizable portion of extracellular Ca^{2+}. We showed that extracellular Ca^{2+} can be efficiently taken up into the ER through the activity of SERCA and from the ER it can be transferred to other compartments like the mitochondria and acidic stores. These activities would ensure that Ca^{2+} is released at specific locations without flooding the whole cell with Ca^{2+}, which may trigger unnecessary signals. Although initial data suggested a less important role for the mitochondria and PLVAC in Ca^{2+} storage, our results showed that these organelles may become more relevant Ca^{2+} reservoirs during ER calcium overload.

The SERCA Ca^{2+}-ATPase is a P-type ATPase found in the membranes of the ER and the secretory pathway (Kuhlbrandt, 2004). The mammalian genome encodes for three SERCA pumps: SERCA1, SERCA2, and SERCA3, and seven different isoforms expressed from these genes, SERCA1a/1b, SERCA2a/2b, and SERCA3a/3b/3c (Periasamy and Kalyanasundaram, 2007). SERCA2b is the most widespread of all isoforms and phylogenetically likely the oldest and considered the house-keeping isoform (Wuytack *et al.*, 2002). SERCA pumps translocate two Ca^{2+} ions and hydrolyze one ATP for each catalytic turnover. This pumping activity serves several roles. By translocating Ca^{2+} from the cytosol into the lumen of the ER, it restores the cytosolic Ca^{2+} concentration to its low resting level (<100 nM). The stored Ca^{2+} can be released and activate many cellular activities. In addition, SERCA maintains a sufficiently high (~500 μM) luminal Ca^{2+} concentration that is necessary for enzyme activities important for proliferation, growth, and differentiation (Wuytack *et al.*, 2002).

T. gondii appears to express a single SERCA protein (TgSERCA) (Nagamune and Sibley, 2006), most likely playing a housekeeping role like the mammalian SERCA2. This was evident from the strong phenotype of the *iΔTgserca* (+ATc) mutant, which could not replicate after 24 h and was defective for all the steps of the tachyzoite lytic cycle. The activity of TgSERCA was highly dependent on the presence of its substrate MgATP and it showed high affinity for Ca^{2+}. Considering the low affinity of the indicator Magfluo4 (Kd: 22 μM), the measured uptake activity

344 and the accumulation of Ca^{2+} was impressive as it was evident even at 55 nM free calcium. This
345 result implied that TgSERCA is active at the cytosolic levels of 60-100 nM Ca^{2+} levels for efficient
346 filling the ER with Ca^{2+}.
347 Ca^{2+} signals are specifically contingent on their spatial, temporal and amplitude features.
348 Movement of Ca^{2+} in the cytosol of cells is severely limited due to the presence of high affinity
349 Ca^{2+} buffers. In mammalian cells it was shown that Ca^{2+} tunnels through the ER as it moves faster
350 because the Ca^{2+} binding capacity of the ER is almost 100 lower than the binding capacity of the
351 cytosol (Mogami *et al.*, 1997). The ER Ca^{2+} transport through its lumen was shown to provide a
352 mechanism of delivering Ca^{2+} to targeted sites without activating inappropriate processes in the
353 cell cytosol (Petersen *et al.*, 2017). In *T. gondii*, the Ca^{2+} binding capacity of the cytosol compared
354 to the ER is less known as the localization of all its predicted Ca^{2+} binding proteins have not been
355 completely determined and several calmodulin-like proteins showed localization to the conoid
356 (Long *et al.*, 2017). In addition, the mechanism (s) of Ca^{2+} entry at the plasma membrane or release
357 from the ER are not fully characterized.
358 In *T. gondii* cytoplasmic Ca^{2+} increases, due to efflux from the ER, have been reported to initiate
359 essential parasite traits like microneme secretion (Carruthers and Sibley, 1999; Nagamune *et al.*,
360 2007b), conoid extrusion (Del Carmen *et al.*, 2009), invasion (Vieira and Moreno, 2000; Lovett
361 and Sibley, 2003) and egress (Arrizabalaga *et al.*, 2004). These responses require precise
362 spatiotemporal control of diverse targets and suggests the presence of distinct systems to deliver
363 Ca^{2+} to specific locations. Our hypothesis is that the ER plays a central role by distributing Ca^{2+} to
364 those locations at specific times for the initiation of parasite functions. The strong invasion,
365 replication and egress phenotypes of the *iΔTgserca* (+ATc) supports this hypothesis.
366 In mammalian cells Ca^{2+} ion is transferred from the ER to the mitochondrion through the outer
367 membrane voltage-dependent anion channel1 (VDAC1) (Gincel *et al.*, 2001; Rapizzi *et al.*, 2002)
368 and the inner membrane calcium uniporter (MCU1) (De Stefani *et al.*, 2011). A VDAC homologue
369 is present in *T. gondii*, which was shown to be essential for growth and for mitochondrial and ER
370 morphology (Mallo *et al.*, 2021). However, the molecular evidence for the presence of a Ca^{2+}
371 uniporter in the inner mitochondrial membrane driven by the electrochemical gradient generated
372 by the electron transport is not supported by the genome database. Calcium transport into the *T.*
373 *gondii* mitochondrion had not been previously shown and our data represents the first experimental
374 evidence showing this event although the molecular mechanism is less clear. We showed that it
375 has very low affinity for Ca^{2+} and it was only possible to observe in intact parasites after inhibiting
376 SERCA, which allowed the increase of the concentration of Ca^{2+} at the local ER membrane. Over
377 the past decade a new concept about the communication between subcellular organelles through
378 tight, stable, and yet non-fusogenic associations known as membrane contact sites (MCSs) has
379 emerged (Phillips and Voeltz, 2016). The ER forms an extensive network of MCSs with the PM,
380 mitochondria and endocytic vesicles for the exchange of Ca^{2+} (Burgoyne *et al.*, 2015).
381 In *T. gondii* the characterization of MCSs is only in its beginnings (Huet and Moreno, 2023) with
382 only a few evidences for their presence (Tomova *et al.*, 2009; Mallo *et al.*, 2021; Ovciarikova *et*
383 *al.*, 2022; Ovciarikova *et al.*, 2024) and function (Li *et al.*, 2021; Oliveira Souza *et al.*, 2022).

384 When *T. gondii* is intracellular, microscopy observations showed that its mitochondrion surrounds
385 the periphery of the cell in a lasso-shape conformation. On the other hand, in extracellular parasites
386 the mitochondrion changes its morphology and adopts a sperm-like or collapsed conformation
387 (Ovciarikova *et al.*, 2017). Our IFA analysis with ER and mitochondrial markers showed that the
388 lasso-shaped mitochondrion surrounds the ER with plenty of opportunities for contact between
389 both organelles. We speculate that at this stage the mitochondrion is buffering any leakage of Ca^{2+}
390 from the ER to prevent premature egress as a cytosolic increase would stimulate motility and
391 possibly egress.
392 In this work, we showed that Ca^{2+} can be transferred from the ER to the mitochondrion, most
393 likely through MCSs as the low affinity of the mitochondrion would not permit uptake directly
394 from the cytosol. Down regulation of TgSERCA resulted in diminished response to acidic stores
395 triggers, which supported that the ER may also be responsible for their filling. The mitochondrion
396 may also be able to take up Ca^{2+} from acidic stores like the PLVAC as GPN was also able to
397 stimulate Ca^{2+} uptake and the response was diminished in the *iΔTgserca* (+ATc) mutant. Transfer
398 of Ca^{2+} from acidic stores to the mitochondrion was impacted by the ER depletion (Fig. 7).
399 In conclusion, this study showed how the ER of *T. gondii* replenish itself with calcium and how
400 it supplies Ca^{2+} to the cytosol for signaling and to acidic stores and the mitochondrion. *T. gondii*
401 is a protozoan parasite that causes disease by reiterating a lytic cycle that is driven by calcium
402 signaling. This work contributes to the understanding of how extracellular and intracellular Ca^{2+}
403 stores work together to sustain the pathologic features of *T. gondii*. Future studies would aim at
404 finding more about the role of Ca^{2+} in mitochondrial and acidic stores functions.
405
406 **Methods**

407 ***Cell Culture***—*Toxoplasma gondii* tachyzoites (RH and *TatiΔku80* strain) were maintained in
408 human telomerase reverse transcriptase immortalized foreskin fibroblasts (hTERT) (Farwell *et al.*,
409 2000) grown in Dulbecco's modified minimal essential media (DMEM) with 1% FBS.
410
411 ***Generation of SERCA mutants***—A promoter insertion plasmid was generated by cloning three
412 PCR fragments into a modified pCR2.1-TOPO vector using Gibson Assembly Cloning Kit (NEB
413 #E5510). One fragment corresponding to the TgSERCA flanking region (predicted
414 promoter/5'UTR) was amplified with primers 1 and 2 (Table S1). The second fragment
415 corresponds to DHFR+T7S4 (Sheiner *et al.*, 2011) and was amplified with primers 3 and 4.
416 Another fragment corresponds to the 5' TgSERCA coding sequence beginning with start codon
417 and was amplified with primers 5 and 6. The vector pCR2.1-TOPO was used, which had only one
418 EcoRI site and it was cut with the enzyme NotI to use as a vector backbone. The promoter insertion
419 plasmid was transfected into the *TatiΔku80* cells and selected with 1 μM pyrimethamine using a
420 "ultra aggressive" screening method. Briefly, 200 μl of the suspension of transfected parasites was
421 added to 10 ml of media and then one to three drops (~65 μl per drop) were inoculated into three
422 24-well plates containing media. The clonal lines created after selection and subcloning were
423 termed *iΔSERCA*.

424 For *in situ* tagging, an approximately 2 kb fragment was amplified from the genomic locus (3'
425 region) of the TgSERCA gene using primers 7 and 8. The fragment was cloned into the pLic-3HA-
426 CAT plasmid (Huynh and Carruthers, 2009) and the construct was linearized with the enzyme
427 NheI for transfection into the *iΔSERCA* mutant. Clonal cell lines were generated after selection
428 with chloramphenicol and subcloning and termed *iΔSERCA-3HA*.
429
430 ***Expression and purification of TgSERCA recombinant protein***—The phosphorylation(P) and
431 nucleotide binding(N) domains of *Tg*SERCA (TGGT1_230420) (nucleotides 1123 to 2415, amino
432 acid residues 375 to 805) were cloned into XmaI and HindIII sites of pQE-80L with primers 13
433 and 14 to create recombinant protein with a N-terminal 6xHis tag. The resulting plasmid was
434 transformed into *Escherichia coli* BL21-CodonPlus competent cells and expression was induced
435 by addition of 0.4 mM isopropyl β-D-1-thiogalactopyranoside (IPTG) for 4 hours at 37ºC. Cells
436 were pelleted and resuspended in equilibration/binding buffer (50 mM Na_3PO_4, 300 mM NaCl, 10
437 mM Imidazole, 8 M Urea, and protease inhibitor cocktail P-8849). The cells were then sonicated
438 for 80 seconds total and centrifuged at 12,000 rpm for 20 mins at 4ºC. The supernatant was filtered
439 through a 0.45 µm membrane and the protein was purified using HisPur Ni-NTA Chromatography
440 Cartridge (Thermo Scientific) following instructions from the manufacturer. Proteins that were
441 unbound were washed off with 12 ml of wash buffer (50 mM Na_3PO_4, 300 mM NaCl, 40 mM
442 imidizole, and 8 M urea), and the recombinant protein was eluted with 5 ml elution buffer (50
443 mM Na_3PO_4 , 300 mM NaCl, 250 mM imidazole, and 8 M urea). Eluted protein fractions were
444 concentrated and desalted with Amicon Ultra-0.5 mL centrifugal filter (Millipore Sigma).
445
446 ***Anti-TgSERCA antibody generation in Guinea pigs***—Two Guinea pigs were each immunized
447 with 0.2 mg of purified recombinant protein mixed with equal volume of Freund's Complete
448 Adjuvant (Sigma F5581), followed by two boosts of 0.1 mg antigen mixed with equal volume of
449 Freund's Incomplete Adjuvant (Sigma F5506) for Guinea pig 1 and three boosts for Guinea pig 2.
450 The resulting antibodies were tested at 1:1000 in western blot against RH lysates and were
451 developed with Alexa Fluor 488 goat anti-Guinea pig (1:1000). The antibodies were compared
452 with Dr. Sibley's mouse anti-SERCA antibody (Nagamune *et al.*, 2007a) to confirm size and
453 purity. The anti-*Tg*SERCA antibodies were then affinity purified.
454
455 ***Cytosolic calcium measurements with Fura-2***—*T. gondii* tachyzoites were loaded with Fura-2
456 AM as previously described (Vella *et al.*, 2020; Stasic *et al.*, 2021). Freshly released tachyzoites
457 were washed twice with buffer A plus glucose (BAG; 116 mM NaCl, 5.4 mM KCl, 0.8 mM
458 MgSO4, 50 mM Hepes, pH 7.3, and 5.5 mM glucose), by centrifugation (706 x *g* for 10 min) and
459 re-suspended to a final density of 1 x $l0^9$ parasites/ml in loading buffer (BAG plus 1.5% sucrose,
460 and 5 µM Fura2 AM). The suspension was incubated for 26 min at 26 °C with mild agitation.
461 Subsequently, the parasites were washed twice (2000 x *g* for 2 min) with BAG to remove
462 extracellular dye, re-suspended to a final density of $1x10^9$ parasites per ml in BAG and kept on
463 ice. For fluorescence measurements, 2 x 10^7 parasites/mL were placed in a cuvette with 2.5 mL of
464 Ringer's buffer without calcium (155 mM NaCl, 3 mM KCl, 1 mM $MgCl_2$, 3 mM NaH_2PO_4, and
465 10 mM Hepes, and 10 mM glucose). Fluorescence measurements were done in an Hitachi F-7000

466 or F-4500 fluorescence spectrophotometer using the Fura-2 conditions for excitation (340 and 380
467 nm) and emission (510 nm). The Fura-2 fluorescence response to Ca^{2+} was calibrated from the
468 ratio of 340/380 nm fluorescence values after subtraction of the background fluorescence of the
469 cells at 340 and 380 nm as previously described (Grynkiewicz *et al.*, 1985). The Ca^{2+} release rate
470 was defined as the change in Ca^{2+} concentration during the initial 20 s after reagent addition. Delta
471 F was calculated by the difference between the higher calcium peak and basal Ca^{2+}, and recovery
472 was defined as the change of Ca^{2+} concentration after the calcium peak was reached for the
473 subsequent indicated times.
474
475 ***Endoplasmic reticulum Ca^{2+} Measurements in permeabilized T. gondii tachyzoites***—
476 Tachyzoites freshly egressed and washed as described above were resuspend to a final density of
477 $1x10^9$ cells/ml in HBS buffer (135 mM NaCl, 5.9 mM KCl, 1.2 mM $MgCl_2$, 11.6 mM HEPES pH
478 7.3, 1.5 mM $CaCl_2$, 11.5 mM glucose) containing 1 mg/ml BSA, 0.2 mg/ml of pluronic F127 and
479 20 μM MagFluo4/AM. The suspension was incubated at RT with mild shaking for 1 h, in the dark.
480 Subsequently, parasites were washed 2 times at 5,000 rpm for 2 min to remove extracellular dye.
481 The pellet was resuspended in 1.8 ml of CLM buffer (20 mM NaCl, 140 mM KCl, 20 mM PIPES,
482 pH 7.0) containing 1 mM EGTA at $1x10^9$ cells/ml. Cells were permeabilized with 44.4 μg/ml
483 digitonin for 6 min. Cells were washed 2 times with CLM containing 1 mM EGTA at 5,000 rpm
484 for 2 min to remove digitonin and resuspended to a final density of $1x10^9$ tachyzoites/ml and kept
485 in ice. For each test, 50 μl ($5x10^7$) of parasite suspension was added to 1.95 ml of CLM containing
486 1 mM EGTA and 0.375 mM $CaCl_2$ which results in 220 nM free Ca^{2+} as calculated with
487 MaxChelator. Fluorescence was measured with an Hitachi F-7000 or F-4500 fluorescence
488 spectrophotometer (Excitation at 485 nm and emission at 520 nm). Ratio ($\Delta F/F_0$) was evaluated
489 by measuring the rate of change in fluorescence over 20 s after reagent addition.
490
491 ***Strain construction and maintenance***—The organelle targeting of GCaMP6f was made by
492 overlapping PCR. The N-terminal mitochondrial targeting sequence of the *T. gondii* SOD2 gene
493 (Pino *et al.*, 2007) was used to target GCaMP6f to the mitochondrion. The Gcamp6f for this
494 construct was amplified by primers 9 and 10 (Table S1). After gel purification of the GCaMP6f
495 and SOD2 sequences, the mitochondria targeting construct was built by overlapping PCR with the
496 purified PCR products as template. This construct was then cloned into the Topo-blunt vector.
497 After the sequence was verified by sequencing, the SOD2-Gcamp6f fragment was removed by
498 BglII and AvrII digestion and cloned into the same restriction sites of the pDT7S4H3 (Sheiner *et*
499 *al.*, 2011) and pCTH3 (Vella *et al.*, 2020) vectors. The pDT7S4H3-SOD2-GCaMP6f construct
500 was introduced into RH parasites by electroporation. After selection with pyrimethamine, the
501 parasites were sorted by FACS and then subcloned. Clones were selected based on the dynamic
502 range of the response to ionomycin. The pCTH3-SOD2-GCaMP6f was introduced into the
503 *iΔTgSERCA* mutant by electroporation. After selection with chloramphenicol, the parasites were
504 sorted by FACS and then subcloned. The expression of GCaMP6f was verified by live cell
505 imaging, IFA, and western blots. The clone with the largest dynamic range, as evaluated with
506 Ionomycin, was selected to further use.
507

508 ***GCaMP6f fluorescence Measurements***—Permeabilized tachyzoites: *T. gondii* tachyzoites
509 expressing SOD2-GCaMP6 were collected and washed 2 times at 5,000 rpm for 2 min with BAG.
510 The parasite pellet was resuspended in 1.8 ml of BAG buffer containing 0.1 mM EGTA at $1x10^9$
511 cells/ml. Permeabilization with 44.4μg/ml digitonin for 6 min was done by following the
512 fluorescence of GCaMP6. Cells were washed 2 times with the same buffer at 5,000 rpm for 2 min
513 to remove digitonin, resuspended to a final density of $1\ x10^9$ parasites/ml in intracellular buffer
514 (140 mM Kgluconate, 10 mM NaCl, 2.7 mM $MgSO_4$, 200 μM EGTA, 65 μM $CaCl_2$, 10 mM
515 Hepes, 10 mM Tris, pH 7.3, 1 mM Glucose) and kept in ice. 50 μl ($5x10^7$) of the parasite
516 suspension was mixed with 1.95 ml intracellular buffer for measurement. Measurements were
517 done in a Hitachi 7000 fluorescence spectrophotometer set at 485 nm excitation and 509 nm
518 emission. The uptake rate ($\Delta F/F_0$/Sec) was evaluated by measuring the % of change in fluorescence
519 per second during the initial 20 s after reagent addition.
520 For measurements with intact parasites, they were collected, washed, and resuspended in BAG
521 at $1x10^9$ cells/ml for testing. 50 μl ($5x10^7$) of the parasite suspension was mixed with 1.95 ml BAG
522 containing 0.1 mM EGTA for measurement. The ratio ($\Delta F/F_0$) was evaluated by measuring the
523 maximum change in fluorescence over 20 s after reagent addition (linear rate).
524
525 ***Growth, Invasion and Egress assays***—Red-green invasion assays were performed as originally
526 described (Kafsack *et al.*, 2004), modified (Chasen *et al.*, 2017) and adapted to use td-RFP
527 expressing parasites. The number of tachyzoites used was 2 x 10^7, and invasion was for 5 min.
528 Plaque assays were performed as described in (Liu *et al.*, 2014) with modifications. 125
529 tachyzoites were used for infection of confluent six well plates with hTert fibroblasts followed by
530 an incubation time of 10 days prior to fixing and staining with crystal violet.
531 For egress assays, the monolayers of hTERT cells grown in 35 mm Mattek dishes were infected
532 with 50,000 tdTomato-expressing parasites. Parasitophorous vacuoles containing 4-8 parasites
533 were observed by microscopy after washing twice with Ringer's buffer without calcium. The dish
534 was filled with 1 ml of Ringer's buffer supplement with either 100 μM EGTA or 1.8 mM $CaCl_2$.
535 Images were collected in time-lapse mode with an acquisition rate of 3 seconds for 15 minutes.
536 We observed that most of the *iΔTgSERCA* cells +/- ATc were still able to egress when stimulated
537 with 1 or 0.5 μM ionomycin added 2 minutes after the start of the recordings with either 100 μM
538 EGTA or 1.8 mM $CaCl_2$. We next used lower concentrations of ionomycin (100 nM and 50 nM)
539 in Ringer"s buffer with 1.8 mM $CaCl_2$ or 0.01% saponin. For egress triggered by ionomycin, the
540 percentage of vacuoles egressed after adding ionomycin during the 15 minutes of the video (2
541 minutes baseline + 13 minutes after adding ionomycin) was quantified. For egress triggered by
542 saponin, the time to egress after adding saponin was quantified.
543 For natural egress, the *iΔTgSERCA* mutant expressing td-tomato RFP was used to infect
544 confluent hTERT cell monolayers 36 hours before adding ATc and 1 μM compound 1 (pyrrole 4-
545 [2-(4-fluorophenyl)-5-(1-methylpiperidine-4-yl)-1H-pyrrol-3-yl]pyridine) (cpd1) (Donald *et al.*,
546 2002) dissolved in ethanol and the culture continued for 24 hours. After treating with cpd1 for 24
547 hours, cultures showed full vacuoles which differed from the vehicle treated plates (36 hours
548 cultured plus ATc treatment for 24 hours or 48 hours without ATc), which were fully lysed. The

549 cpd1 media was removed and the synchronized vacuoles were washed twice, and the media
550 replaced with media without cpd1. The plates were then moved to the prewarmed DeltaVision
551 microscope for observation. After 10 minutes at 37 C, egress of the full vacuoles was enumerated.
552 We counted each plate for 1 minute and we counted at least 100 vacuoles per experiment. 3
553 independent biological experiments were conducted and summarized.
554 For replication assays, the hTERT cells were grown on 35 mm Mattek dishes. Each dish was
555 infected with 50,000 tdTomato-expressing parasites. 24 h after the infection the counting of
556 parasites per PV was done in a fluorescence microscope. For each experiment, at least 100 PVs
557 were counted. Results were the average of 3 independents experiments (Li *et al.*, 2021).
558
559 ***Microscopy and western blot analyses***—Tachyzoites were grown on hTERT cells on cover slips for
560 ~24 hr, washed twice with BAG and fixed with 4% formaldehyde for 1 h, followed by
561 permeabilization with 0.3% Triton X-100 for 20 min, and blocking with 3% bovine serum albumin.
562 IFAs were performed as previously described (Miranda *et al.*, 2010). Fluorescence images were
563 collected with an Olympus IX-71 inverted fluorescence microscope with a Photometrix CoolSnapHQ
564 CCD camera driven by DeltaVision software (Applied Precision, Seattle, WA). Superresolution
565 microscopy was performed using a Zeiss ELYRA S1 (SR-SIM) microscope with a high-resolution
566 Axio observer Z1 inverted microscope stand with transmitted (HAL), UV (HBO,) and high-power
567 solid-state laser illumination sources (405/488/561 nm), a 100x oil immersion objective, and an Andor
568 iXon EM-CCD camera and acquired using the ZEN software (Zeiss) with a SIM analysis module.
569 Rat anti-HA antibody from Roche was used at a dilution of 1:25. Mouse anti-HA antibody from
570 Covance was used at a dilution of 1:200. The affinity purified guinea pig anti-TgSERCA activity was
571 used at 1:500 dilution.
572 Western blot analysis was performed as previously described (Liu *et al.*, 2014). Rat anti-HA
573 antibody from Roche was used at a dilution of 1:200. Mouse anti-HA antibody from Covance was
574 used at a dilution of 1:1,000. The guinea pig anti-TgSERCA antibody was used at a dilution of 1:2000.
575 Secondary goat anti-rat or mouse antibody conjugated with HRP was used at 1:5,000. Mouse anti-α-
576 tubulin at a dilution of 1:5,000 was used for loading control.
577
578 ***Transmission Electron Microscopy***—For ultrastructural observations of intracellular *T. gondii* by
579 thin-section transmission electron microscopy (EM), infected human foreskin fibroblast cells were
580 fixed in 2.5% glutaraldehyde in 0.1 mM sodium cacodylate (EMS) and processed as described
581 (Coppens and Joiner, 2003). Ultrathin sections of infected host cells were stained before examination
582 with a Hitachi 7600 EM under 80 kV. For quantitative measurement of distance between organelles,
583 the closest point between *T. gondii's* organelles and ER membrane was measured using ImageJ and
584 was performed on 47 representative electron micrographs at the same magnification for accurate
585 comparison between organelles
586
587 ***Statistical Analysis***—Statistical analyses were performed by Student's t-test using GraphPad PRISM
588 version 9. Error bars shown represent mean ± SD (standard deviation) of at least three independent
589 biological replicates. Unpaired two tailed t test performed in all comparisons.
590

Acknowledgments

The authors thank Dr. Muthugapatti Kandasamy and the Biomedical Microscopy Core of the University of Georgia for the use of the microscopes. The CTEGD Cytometry Shared Resource Laboratory provided access and training to state-of-the-art flow cytometry analyzers. We would like to thank David Sibley for the generous gift of the mouse SERCA antibody and the plasmid for SERCA expression. This work was supported by the U.S. National Institutes of Health grants AI128356, AI154931 and AI174600 to SNJM and R01AI166921 to IC.

References

Arrizabalaga, G., and Boothroyd, J.C. (2004). Role of calcium during Toxoplasma gondii invasion and egress. International journal for parasitology *34*, 361-368.

Arrizabalaga, G., Ruiz, F., Moreno, S., and Boothroyd, J.C. (2004). Ionophore-resistant mutant of Toxoplasma gondii reveals involvement of a sodium/hydrogen exchanger in calcium regulation. J Cell Biol *165*, 653-662.

Bers, D.M., Patton, C.W., and Nuccitelli, R. (1994). A practical guide to the preparation of Ca2+ buffers. Methods Cell Biol *40*, 3-29.

Bisio, H., and Soldati-Favre, D. (2019). Signaling Cascades Governing Entry into and Exit from Host Cells by Toxoplasma gondii. Annu Rev Microbiol *73*, 579-599.

Black, M.W., and Boothroyd, J.C. (2000). Lytic cycle of Toxoplasma gondii. Microbiol Mol Biol Rev *64*, 607-623.

Blader, I.J., Coleman, B.I., Chen, C.T., and Gubbels, M.J. (2015). Lytic Cycle of Toxoplasma gondii: 15 Years Later. Annu Rev Microbiol *69*, 463-485.

Bootman, M.D., and Bultynck, G. (2020). Fundamentals of Cellular Calcium Signaling: A Primer. Cold Spring Harb Perspect Biol *12*.

Borges-Pereira, L., Budu, A., McKnight, C.A., Moore, C.A., Vella, S.A., Hortua Triana, M.A., Liu, J., Garcia, C.R., Pace, D.A., and Moreno, S.N. (2015). Calcium Signaling throughout the Toxoplasma gondii Lytic Cycle: A STUDY USING GENETICALLY ENCODED CALCIUM INDICATORS. J Biol Chem *290*, 26914-26926.

Burgoyne, T., Patel, S., and Eden, E.R. (2015). Calcium signaling at ER membrane contact sites. Biochim Biophys Acta *1853*, 2012-2017.

Camello, C., Lomax, R., Petersen, O.H., and Tepikin, A.V. (2002). Calcium leak from intracellular stores--the enigma of calcium signalling. Cell Calcium *32*, 355-361.

Carruthers, V.B., and Sibley, L.D. (1999). Mobilization of intracellular calcium stimulates microneme discharge in Toxoplasma gondii. Mol Microbiol *31*, 421-428.

Chasen, N.M., Asady, B., Lemgruber, L., Vommaro, R.C., Kissinger, J.C., Coppens, I., and Moreno, S.N.J. (2017). A Glycosylphosphatidylinositol-Anchored Carbonic Anhydrase-Related Protein of Toxoplasma gondii Is Important for Rhoptry Biogenesis and Virulence. mSphere *2*.

Chen, T.W., Wardill, T.J., Sun, Y., Pulver, S.R., Renninger, S.L., Baohan, A., Schreiter, E.R., Kerr, R.A., Orger, M.B., Jayaraman, V., Looger, L.L., Svoboda, K., and Kim, D.S. (2013). Ultrasensitive fluorescent proteins for imaging neuronal activity. Nature *499*, 295-300.

Clapham, D.E. (2007). Calcium signaling. Cell *131*, 1047-1058.

Coppens, I., and Joiner, K.A. (2003). Host but not parasite cholesterol controls Toxoplasma cell entry by modulating organelle discharge. Mol Biol Cell *14*, 3804-3820.

De Stefani, D., Raffaello, A., Teardo, E., Szabo, I., and Rizzuto, R. (2011). A forty-kilodalton protein of the inner membrane is the mitochondrial calcium uniporter. Nature *476*, 336-340.

Del Carmen, M.G., Mondragon, M., Gonzalez, S., and Mondragon, R. (2009). Induction and regulation of conoid extrusion in Toxoplasma gondii. Cell Microbiol *11*, 967-982.

Donald, R.G., Allocco, J., Singh, S.B., Nare, B., Salowe, S.P., Wiltsie, J., and Liberator, P.A. (2002). Toxoplasma gondii cyclic GMP-dependent kinase: chemotherapeutic targeting of an essential parasite protein kinase. Eukaryot Cell *1*, 317-328.

Endo, T., Sethi, K.K., and Piekarski, G. (1982). Toxoplasma gondii: calcium ionophore A23187-mediated exit of trophozoites from infected murine macrophages. Exp Parasitol *53*, 179-188.

Farwell, D.G., Shera, K.A., Koop, J.I., Bonnet, G.A., Matthews, C.P., Reuther, G.W., Coltrera, M.D., McDougall, J.K., and Klingelhutz, A.J. (2000). Genetic and epigenetic changes in human epithelial cells immortalized by telomerase. Am J Pathol *156*, 1537-1547.

Gincel, D., Zaid, H., and Shoshan-Barmatz, V. (2001). Calcium binding and translocation by the voltage-dependent anion channel: a possible regulatory mechanism in mitochondrial function. The Biochemical journal *358*, 147-155.

Grynkiewicz, G., Poenie, M., and Tsien, R.Y. (1985). A new generation of Ca2+ indicators with greatly improved fluorescence properties. J Biol Chem *260*, 3440-3450.

Hager, K.M., Striepen, B., Tilney, L.G., and Roos, D.S. (1999). The nuclear envelope serves as an intermediary between the ER and Golgi complex in the intracellular parasite Toxoplasma gondii. J Cell Sci *112 (Pt 16)*, 2631-2638.

Haller, T., Dietl, P., Deetjen, P., and Volkl, H. (1996). The lysosomal compartment as intracellular calcium store in MDCK cells: a possible involvement in InsP3-mediated Ca2+ release. Cell Calcium *19*, 157-165.

Hortua Triana, M.A., Marquez-Nogueras, K.M., Fazli, M.S., Quinn, S., and Moreno, S.N.J. (2024). Regulation of calcium entry by cyclic GMP signaling in Toxoplasma gondii. J Biol Chem *300*, 105771.

Hortua Triana, M.A., Marquez-Nogueras, K.M., Vella, S.A., and Moreno, S.N.J. (2018). Calcium signaling and the lytic cycle of the Apicomplexan parasite Toxoplasma gondii. Biochim Biophys Acta Mol Cell Res *1865*, 1846-1856.

Huet, D., and Moreno, S.N.J. (2023). Interorganellar Communication Through Membrane Contact Sites in Toxoplasma Gondii. Contact (Thousand Oaks) *6*, 25152564231189064.

Huynh, M.H., and Carruthers, V.B. (2009). Tagging of endogenous genes in a Toxoplasma gondii strain lacking Ku80. Eukaryot Cell *8*, 530-539.

Kafsack, B.F., Beckers, C., and Carruthers, V.B. (2004). Synchronous invasion of host cells by Toxoplasma gondii. Mol Biochem Parasitol *136*, 309-311.

Kuhlbrandt, W. (2004). Biology, structure and mechanism of P-type ATPases. Nat Rev Mol Cell Biol *5*, 282-295.

Li, Z.H., King, T.P., Ayong, L., Asady, B., Cai, X., Rahman, T., Vella, S.A., Coppens, I., Patel, S., and Moreno, S.N.J. (2021). A plastid two-pore channel essential for inter-organelle communication and growth of Toxoplasma gondii. Nat Commun *12*, 5802.

Liu, J., Pace, D., Dou, Z., King, T.P., Guidot, D., Li, Z.H., Carruthers, V.B., and Moreno, S.N. (2014). A vacuolar-H(+) -pyrophosphatase (TgVP1) is required for microneme secretion, host cell invasion, and extracellular survival of Toxoplasma gondii. Mol Microbiol *93*, 698-712.

Lloyd-Evans, E., Morgan, A.J., He, X., Smith, D.A., Elliot-Smith, E., Sillence, D.J., Churchill, G.C., Schuchman, E.H., Galione, A., and Platt, F.M. (2008). Niemann-Pick disease type C1 is a sphingosine storage disease that causes deregulation of lysosomal calcium. Nat Med *14*, 1247-1255.

Long, S., Brown, K.M., Drewry, L.L., Anthony, B., Phan, I.Q.H., and Sibley, L.D. (2017). Calmodulin-like proteins localized to the conoid regulate motility and cell invasion by Toxoplasma gondii. PLoS Pathog *13*, e1006379.

Lourido, S., and Moreno, S.N. (2015). The calcium signaling toolkit of the Apicomplexan parasites Toxoplasma gondii and Plasmodium spp. Cell Calcium *57*, 186-193.
Lovett, J.L., and Sibley, L.D. (2003). Intracellular calcium stores in Toxoplasma gondii govern invasion of host cells. J Cell Sci *116*, 3009-3016.
Luo, S., Ruiz, F.A., and Moreno, S.N. (2005). The acidocalcisome Ca2+-ATPase (TgA1) of Toxoplasma gondii is required for polyphosphate storage, intracellular calcium homeostasis and virulence. Mol Microbiol *55*, 1034-1045.
Luo, S., Vieira, M., Graves, J., Zhong, L., and Moreno, S.N. (2001). A plasma membrane-type Ca(2+)-ATPase co-localizes with a vacuolar H(+)-pyrophosphatase to acidocalcisomes of Toxoplasma gondii. EMBO J *20*, 55-64.
Mallo, N., Ovciarikova, J., Martins-Duarte, E.S., Baehr, S.C., Biddau, M., Wilde, M.L., Uboldi, A.D., Lemgruber, L., Tonkin, C.J., Wideman, J.G., Harding, C.R., and Sheiner, L. (2021). Depletion of a Toxoplasma porin leads to defects in mitochondrial morphology and contacts with the endoplasmic reticulum. J Cell Sci *134*.
Marquez-Nogueras, K.M., Hortua Triana, M.A., Chasen, N.M., Kuo, I.Y., and Moreno, S.N. (2021). Calcium signaling through a transient receptor channel is important for Toxoplasma gondii growth. Elife *10*.
Miranda, K., Pace, D.A., Cintron, R., Rodrigues, J.C., Fang, J., Smith, A., Rohloff, P., Coelho, E., de Haas, F., de Souza, W., Coppens, I., Sibley, L.D., and Moreno, S.N. (2010). Characterization of a novel organelle in Toxoplasma gondii with similar composition and function to the plant vacuole. Mol Microbiol *76*, 1358-1375.
Mogami, H., Nakano, K., Tepikin, A.V., and Petersen, O.H. (1997). Ca2+ flow via tunnels in polarized cells: recharging of apical Ca2+ stores by focal Ca2+ entry through basal membrane patch. Cell *88*, 49-55.
Moreno, S.N., and Zhong, L. (1996). Acidocalcisomes in Toxoplasma gondii tachyzoites. The Biochemical journal *313 (Pt 2)*, 655-659.
Nagamune, K., Beatty, W.L., and Sibley, L.D. (2007a). Artemisinin induces calcium-dependent protein secretion in the protozoan parasite Toxoplasma gondii. Eukaryot Cell *6*, 2147-2156.
Nagamune, K., Moreno, S.N., and Sibley, L.D. (2007b). Artemisinin-resistant mutants of Toxoplasma gondii have altered calcium homeostasis. Antimicrob Agents Chemother *51*, 3816-3823.
Nagamune, K., and Sibley, L.D. (2006). Comparative genomic and phylogenetic analyses of calcium ATPases and calcium-regulated proteins in the apicomplexa. Mol Biol Evol *23*, 1613-1627.
Oliveira Souza, R.O., Jacobs, K.N., Back, P.S., Bradley, P.J., and Arrizabalaga, G. (2022). IMC10 and LMF1 mediate mitochondrial morphology through mitochondrion-pellicle contact sites in Toxoplasma gondii. J Cell Sci *135*.
Ovciarikova, J., Lemgruber, L., Stilger, K.L., Sullivan, W.J., and Sheiner, L. (2017). Mitochondrial behaviour throughout the lytic cycle of Toxoplasma gondii. Sci Rep *7*, 42746.
Ovciarikova, J., Shikha, S., Lacombe, A., Courjol, F., McCrone, R., Hussain, W., Maclean, A., Lemgruber, L., Martins-Duarte, E.S., Gissot, M., and Sheiner, L. (2024). Two ancient membrane pores mediate mitochondrial-nucleus membrane contact sites. J Cell Biol *223*.
Ovciarikova, J., Shikha, S., and Sheiner, L. (2022). Nuclear Interactions: A Spotlight on Nuclear Mitochondrial Membrane Contact Sites. Contact (Thousand Oaks) *5*, 25152564221096217.

Pace, D.A., McKnight, C.A., Liu, J., Jimenez, V., and Moreno, S.N. (2014). Calcium entry in Toxoplasma gondii and its enhancing effect of invasion-linked traits. J Biol Chem *289*, 19637-19647.

Papp, S., Dziak, E., Michalak, M., and Opas, M. (2003). Is all of the endoplasmic reticulum created equal? The effects of the heterogeneous distribution of endoplasmic reticulum Ca2+-handling proteins. J Cell Biol *160*, 475-479.

Periasamy, M., and Kalyanasundaram, A. (2007). SERCA pump isoforms: their role in calcium transport and disease. Muscle Nerve *35*, 430-442.

Petersen, O.H., Courjaret, R., and Machaca, K. (2017). Ca(2+) tunnelling through the ER lumen as a mechanism for delivering Ca(2+) entering via store-operated Ca(2+) channels to specific target sites. J Physiol *595*, 2999-3014.

Phillips, M.J., and Voeltz, G.K. (2016). Structure and function of ER membrane contact sites with other organelles. Nat Rev Mol Cell Biol *17*, 69-82.

Pino, P., Foth, B.J., Kwok, L.Y., Sheiner, L., Schepers, R., Soldati, T., and Soldati-Favre, D. (2007). Dual targeting of antioxidant and metabolic enzymes to the mitochondrion and the apicoplast of Toxoplasma gondii. PLoS Pathog *3*, e115.

Rapizzi, E., Pinton, P., Szabadkai, G., Wieckowski, M.R., Vandecasteele, G., Baird, G., Tuft, R.A., Fogarty, K.E., and Rizzuto, R. (2002). Recombinant expression of the voltage-dependent anion channel enhances the transfer of Ca2+ microdomains to mitochondria. J Cell Biol *159*, 613-624.

Rossi, A.M., and Taylor, C.W. (2020). Reliable measurement of free Ca(2+) concentrations in the ER lumen using Mag-Fluo-4. Cell Calcium *87*, 102188.

Sagara, Y., and Inesi, G. (1991). Inhibition of the sarcoplasmic reticulum Ca2+ transport ATPase by thapsigargin at subnanomolar concentrations. J Biol Chem *266*, 13503-13506.

Scorrano, L., De Matteis, M.A., Emr, S., Giordano, F., Hajnoczky, G., Kornmann, B., Lackner, L.L., Levine, T.P., Pellegrini, L., Reinisch, K., Rizzuto, R., Simmen, T., Stenmark, H., Ungermann, C., and Schuldiner, M. (2019). Coming together to define membrane contact sites. Nat Commun *10*, 1287.

Sheiner, L., Demerly, J.L., Poulsen, N., Beatty, W.L., Lucas, O., Behnke, M.S., White, M.W., and Striepen, B. (2011). A systematic screen to discover and analyze apicoplast proteins identifies a conserved and essential protein import factor. PLoS Pathog *7*, e1002392.

Smith, J.B., Zheng, T., and Lyu, R.M. (1989). Ionomycin releases calcium from the sarcoplasmic reticulum and activates Na+/Ca2+ exchange in vascular smooth muscle cells. Cell Calcium *10*, 125-134.

Spang, A. (2018). The endoplasmic reticulum-the caring mother of the cell. Curr Opin Cell Biol *53*, 92-96.

Stasic, A.J., Dykes, E.J., Cordeiro, C.D., Vella, S.A., Fazli, M.S., Quinn, S., Docampo, R., and Moreno, S.N.J. (2021). Ca(2+) entry at the plasma membrane and uptake by acidic stores is regulated by the activity of the V-H(+) -ATPase in Toxoplasma gondii. Mol Microbiol *115*, 1054-1068.

Thastrup, O., Cullen, P.J., Drobak, B.K., Hanley, M.R., and Dawson, A.P. (1990). Thapsigargin, a tumor promoter, discharges intracellular Ca2+ stores by specific inhibition of the endoplasmic reticulum Ca2(+)-ATPase. Proc Natl Acad Sci U S A *87*, 2466-2470.

Tomavo, S., Slomianny, C., Meissner, M., and Carruthers, V.B. (2013). Protein trafficking through the endosomal system prepares intracellular parasites for a home invasion. PLoS Pathog *9*, e1003629.

Tomova, C., Humbel, B.M., Geerts, W.J., Entzeroth, R., Holthuis, J.C., and Verkleij, A.J. (2009). Membrane contact sites between apicoplast and ER in Toxoplasma gondii revealed by electron tomography. Traffic *10*, 1471-1480.

Vella, S.A., Calixto, A., Asady, B., Li, Z.H., and Moreno, S.N.J. (2020). Genetic Indicators for Calcium Signaling Studies in Toxoplasma gondii. Methods Mol Biol *2071*, 187-207.

Vella, S.A., Moore, C.A., Li, Z.H., Hortua Triana, M.A., Potapenko, E., and Moreno, S.N.J. (2021). The role of potassium and host calcium signaling in Toxoplasma gondii egress. Cell Calcium *94*, 102337.

Vieira, M.C., and Moreno, S.N. (2000). Mobilization of intracellular calcium upon attachment of Toxoplasma gondii tachyzoites to human fibroblasts is required for invasion. Mol Biochem Parasitol *106*, 157-162.

Weiss, L.M., and Dubey, J.P. (2009). Toxoplasmosis: A history of clinical observations. Int J Parasitol *39*, 895-901.

Wenzel, E.M., Elfmark, L.A., Stenmark, H., and Raiborg, C. (2022). ER as master regulator of membrane trafficking and organelle function. J Cell Biol *221*.

Wuytack, F., Raeymaekers, L., and Missiaen, L. (2002). Molecular physiology of the SERCA and SPCA pumps. Cell Calcium *32*, 279-305.

Yuan, Y., Kilpatrick, B.S., Gerndt, S., Bracher, F., Grimm, C., Schapira, A.H., and Patel, S. (2021). The lysosomotrope GPN mobilises Ca(2+) from acidic organelles. J Cell Sci *134*.

FIGURES AND FIGURE LEGENDS:

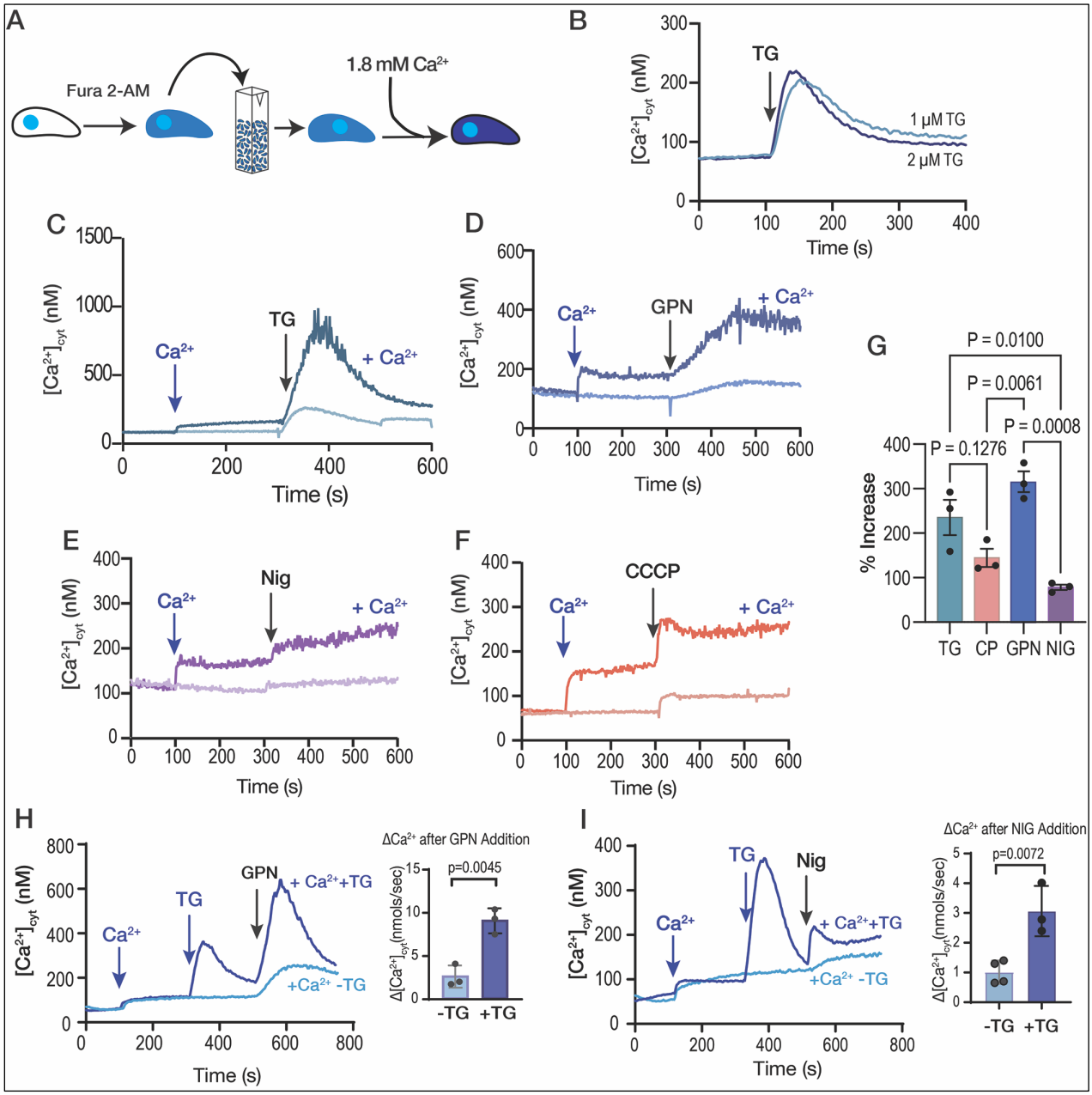

Figure 1: The role of extracellular calcium in the filling of intracellular stores. A, scheme depicting the Fura-2-AM loading and the experimental set-up. **B**, *T. gondii* tachyzoites loaded with Fura-2 were in suspension in Ringer buffer with 100 µM EGTA. Thapsigargin (TG) was added at 100 seconds, at two different concentrations (1 and 2 µM). **C**, Similar experimental set-up to the one shown in B. 1.8 mM $CaCl_2$ was added to the suspension at 100 sec, followed by 2 µM TG at 300 sec (*dark blue trace*). The light blue trace shows the same experiment without the addition of $CaCl_2$. **D**, similar to C but using 40 µM GPN instead of TG. **E**, same experimental set-up to the one shown in C but adding the potassium ionophore nigericin, 10 µM. **F**, same experimental set-up to the one

shown in C but using the mitochondrial uncoupler CCCP. **G**, quantification of the % increase of cytoplasmic calcium by adding extracellular calcium prior to each indicated reagent (TG, thapsigargin; CP, CCCP; NIG, nigericin). **H**, cytosolic calcium measurements following the addition of 1.8 mM extracellular calcium, 1 μM TG prior to the addition of GPN, 40 μM. **I**, cytosolic Calcium measurements following the addition of 1.8 mM extracellular Calcium, 1 μM TG prior to the addition of 10 μM NIG. The quantification shows the comparison of the cytosolic increase with and without the addition of TG. Data are presented as mean ± SD for G, H and I. *p value*: unpaired two tailed t test performed in all comparisons.

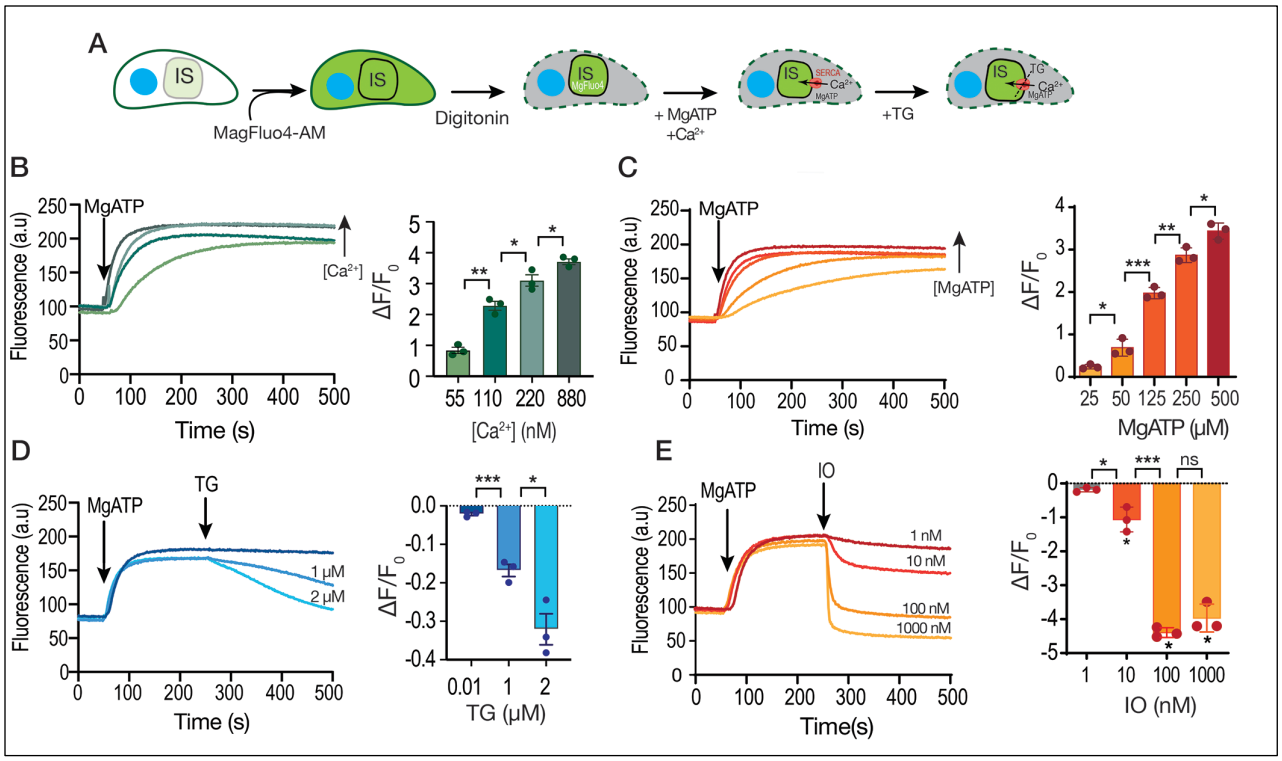

Figure 2: Ca^{2+} uptake by intracellular stores. A, Scheme showing the loading with MagFluo4-AM followed by permeabilization with digitonin of a *T. gondii* tachyzoite (RH parental strain) suspension (IS, intracellular store). **B**, Fluorescence measurements (see Materials and Methods for specifics) of the suspension of parasites loaded with MagFluo4. MgATP was added at 500 μM at 50 seconds. The bar graph shows the quantification of the slope of the increase in fluorescence after adding the SERCA substrate MgATP. The concentration of free calcium was varied, and it is indicated. The calculation of free calcium was done with MaxChelator. **C**, similar experimental set-up to the one shown in B but the concentration of MgATP was varied at the concentrations indicated in the bar graph. Quantification of the slope of fluorescence increase after adding MgATP is shown in the bar graph. **D**, this experiment was done with 500 μM MgATP and 220 nM $CaCl_2$. Thapsigargin (TG) was added to inhibit SERCA causing calcium to be released from the store. The concentrations used are indicated. The bar graph shows the negative slope after the addition of TG. **E**, similar to D, but adding ionomycin (IO). The concentrations used are indicated and the slopes were measured after the addition of IO. Data are presented as mean ± SD for B-D. *p value*: unpaired two tailed t test performed in all comparisons.

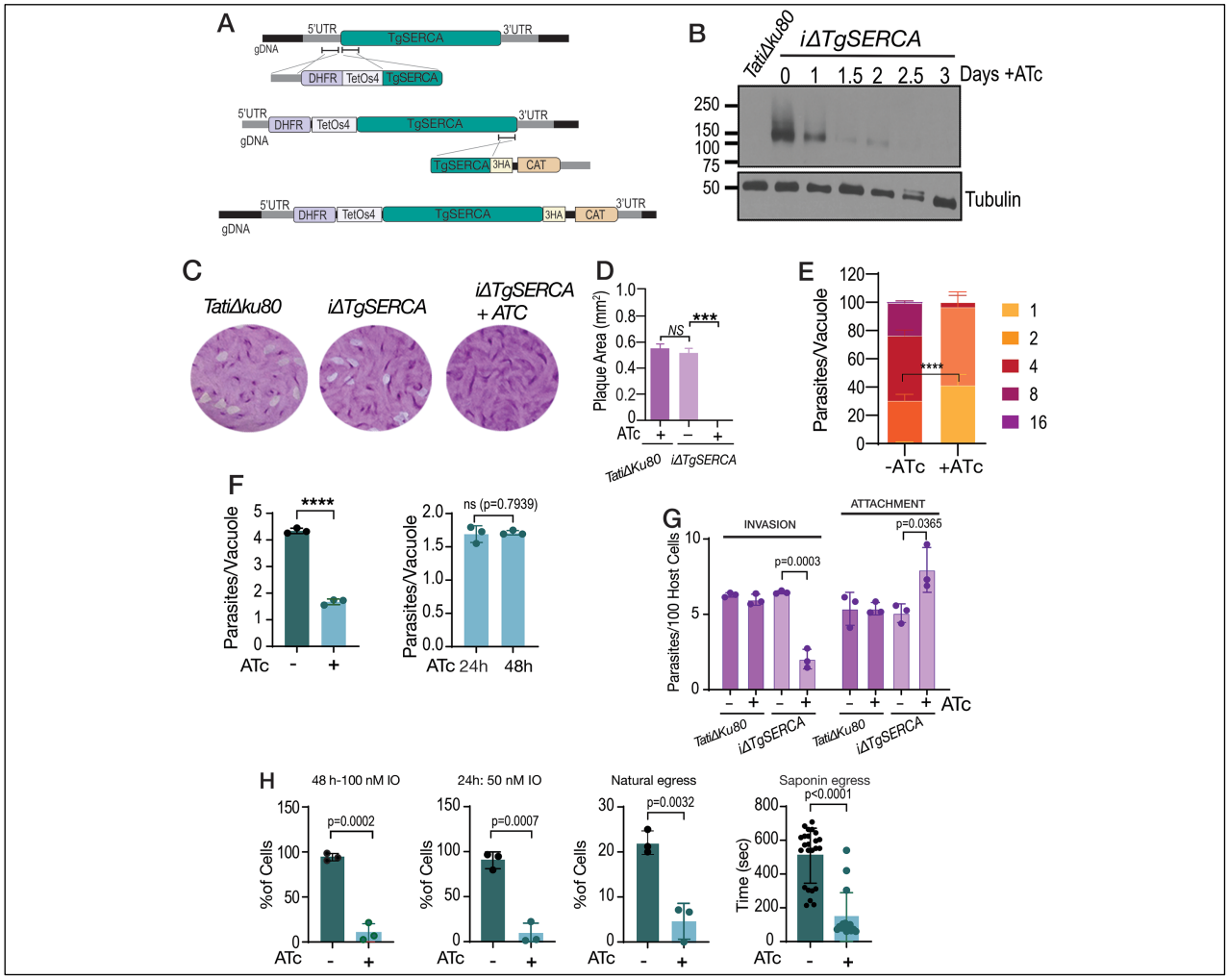

Figure 3: The sarcoplasmic-endoplasmic reticulum calcium ATPase (SERCA) is essential for *T. gondii* replication. A, Scheme showing the strategy used for the down regulation of the expression of TgSERCA by promoter insertion and regulation by 0.5 µg/ml Anhydrotetracyclin (ATc). The mutants generated were termed *iΔTgSERCA* or *iΔTgSERCA-HA* for the C-terminal tagged one. DHFR, Dihydrofolate reductase gene for selection with pyrimethamine; CAT, chloramphenicol acetyl transferase gene for selection with chloramphenicol. **B**, Western blots of *iΔTgSERCA-HA* lysates grown with and without ATc. The expression of TgSERCA is shown by the signal obtained with the anti-HA antibody. **C**, plaque assays comparing the size of plaques formed by tachyzoites (150/well) of the *iΔTgSERCA* mutant grown with and without 0.5 µg/ml ATc for 8 days. Plaques formed by the parental strain *TatiΔku80* are shown for comparison. **D**, quantification of the size of the plaques presented in C. **E**, replication assays using the *iΔTgSERCA_RFP* mutant. Number of parasites per parasitophorous vacuole (PV) obtained 24 h after infection of fibroblast cells is reported and compared between the mutant grown with and without 0.5 µg/ml ATc. Data represented as mean ± SD. *p value*: unpaired two tailed t test performed in all comparisons. **F**, Average number of parasites

per PV counted at 24 h after the initial infection. The graph shown to the right shows the number of parasites per PV of the *iΔTgSERCA* (+ATc) for 24 or 48 hours after the initial infection. **G**, Invasion assays with the *iΔTgSERCA* mutant treated with ATc for 24 h were done using the red-green assay. **H**, Egress assays with the *iΔTgSERCA* mutant previously grown with or without ATc. Egress was triggered with IO (100 or 50 nM) or saponin (0.01%). The protocol for natural egress uses compound 1 and it is detailed in the methods section.

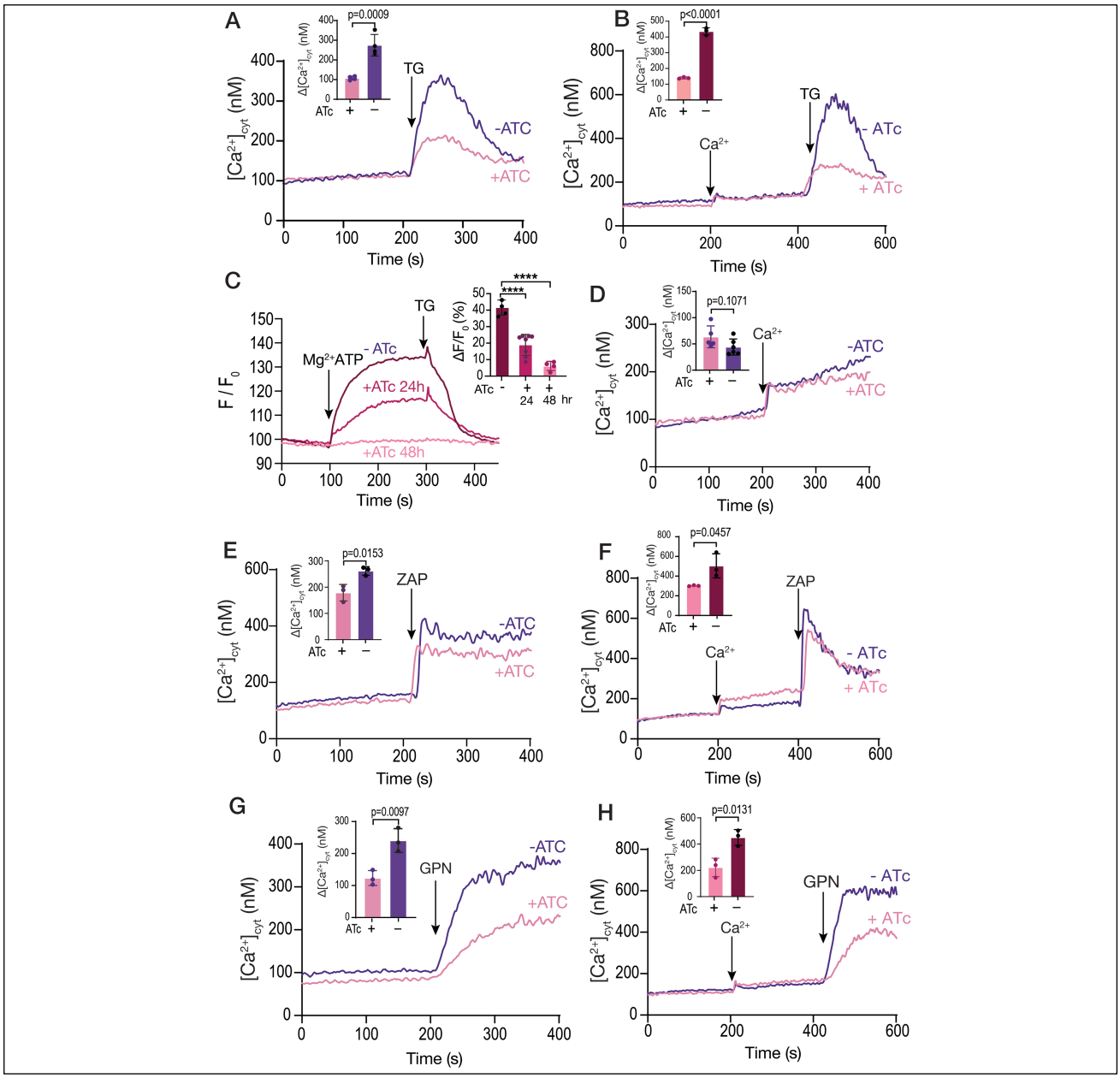

Figure 4: Organellar calcium pools in the *iΔTgserca* mutant. **A**, cytosolic calcium response to the addition of 1 µM TG. The *iΔTgserca* grown with and without ATc was previously loaded with Fura-2 and the cytosolic Ca^{2+} responses were measured. 1 µM TG was added at 200 sec. The purple trace shows the response of the parental cell line grown without ATc and the pink one shows the response of the same mutant grown with ATc for 24 h. The bar graph shows the analysis of the $\Delta[Ca^{2+}]$ from three independent experiments. **B**, same experimental set-up as the one in A but adding 1.8 mM extracellular Ca^{2+} at 200 sec. **C**, SERCA activity measured with MagFluo4-loaded tachyzoites of

iΔTgserca mutant previously grown with or without ATc. Parasites were collected and loaded with MagFluo4-AM as described in the Methods section. Digitonin permeabilized parasites were used in the experiment. The concentration of free calcium in the buffer is 220 nM and MgATP (0.125 mM) was added at 100 sec. The response of the control mutant grown without ATc is shown in purple. The other traces show the response of the mutant grown for either 24 or 48 h with ATc. TG was added at 1 μM TG. The bar graph shows the quantification of the slope after adding MgATP. **D**. Ca^{2+} entry measured in Fura-2 loaded *iΔTgSERCA* (±ATc). 1.8 mM extracellular Ca^{2+} was added at 200 sec. The inset shows the ΔF measurement from three independent experiments and showed no significant difference. **E**, Similar conditions to the ones used in A but adding 100 μM Zaprinast. The bar graph shows the analysis of the $\Delta[Ca^{2+}]$ from three independent experiments. **F**, Similar conditions to the ones used in B but adding 1.8 mM extracellular calcium at 200 sec and 100 μM Zaprinast at 400 sec. The bar graph shows the analysis of the $\Delta[Ca^{2+}]$ from 3 independent experiments. **G**, Same as A but adding 40 μM GPN. The bar graph shows the analysis of the $\Delta[Ca^{2+}]$ from three independent experiments. **H**, Same set-up as in F but adding 1.8 mM Ca^{2+} at 200 sec followed by 40 μM GPN. The bar graph shows the analysis of the $\Delta[Ca^{2+}]$ from three independent experiments. Data are presented as mean ± SD. *p* value: unpaired two tailed t test performed in all comparisons.

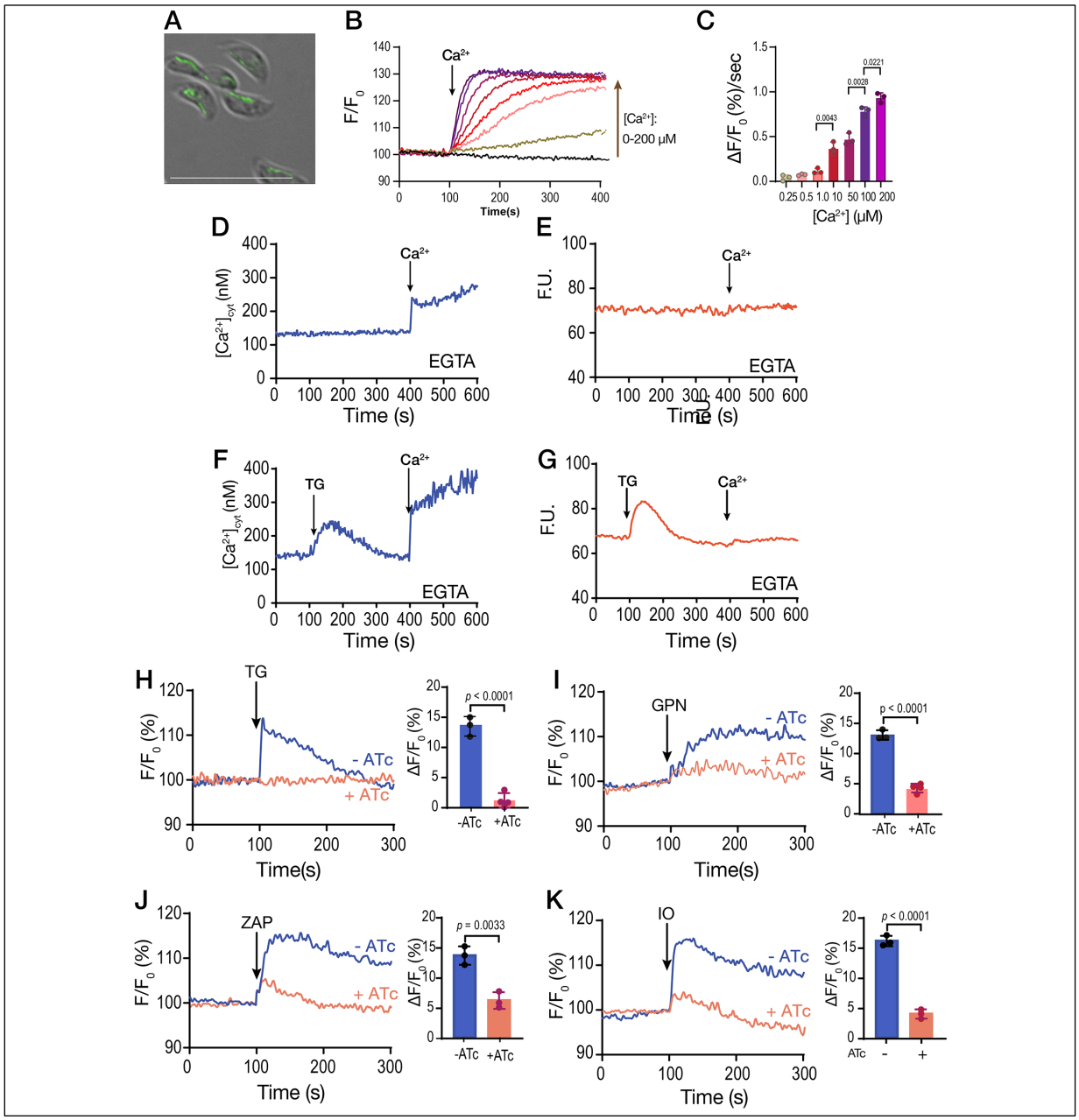

Figure 5: Mitochondrial Calcium uptake. **A**, Fluorescence image of *T. gondii* tachyzoites expressing *SOD2-GCaMP6f* (pDT7S4H3-SOD2-GCaMP6f). The generation of this cell line is described in material and methods. **B**, *T. gondii* tachyzoites expressing SOD2-GCaMP6f ($5x10^7$) permeabilized with digitonin as described in the method's section were tested in a buffer with 100 μM EGTA. Ca^{2+} was added at 100 sec to achieve the final concentrations of 0.25, 0.5, 1, 10, 50, 100 and 200 μM. Maxchelator was used to calculate the final concentrations of free Calcium. **C**, ΔF was measured as the change in fluorescence between the baseline and the maximum obtained 20 sec after the addition of Ca^{2+} from three independent biological experiments. **D**, Fura-2 loaded tachyzoites of

the SOD2-GCaMP6f expressing mutant in suspension. The experimental set-up was identical to the one described in Fig. 1A-B. 1.8 mM $CaCl_2$ was added at 400 sec. Fluorescence measurements were done using the conditions for Fura-2. **E**, GCaMP6 fluorescence measurements of parasites expression SOD2-GCaMP6f in their mitochondrion. The fluorometer conditions were set to measure GCaMP6. **F**, 1 μM TG was added at 100 sec followed by 1.8 mM $CaCl_2$ at 400 sec. Fura2 loaded parasites and Fura2 conditions were used. **G**, Same additions as in F but measuring fluorescence of GCaMP6. **H**, Response to the addition of 1 μM TG of the *iΔTgserca-sod2-gcamp6f* mutant (transfected with pCTH3-SOD2-GCaMP6f plasmid) previously grown in the presence (*pink trace*) or absence (*blue trace*) of ATc. The conditions for the fluorescence measurements are the same used in part G with intact parasites. The bar graph shows the ΔF measurements from three independent experiments. **I**, same as H but using 40 μM GPN. **J**, Same as H but using 100 μM Zaprinast. **K**, Same as H but using 1 μM Ionomycin. Data are presented as mean ± SD from 3 independent biological experiments. *p value*: unpaired two tailed t test performed in all comparisons.

F

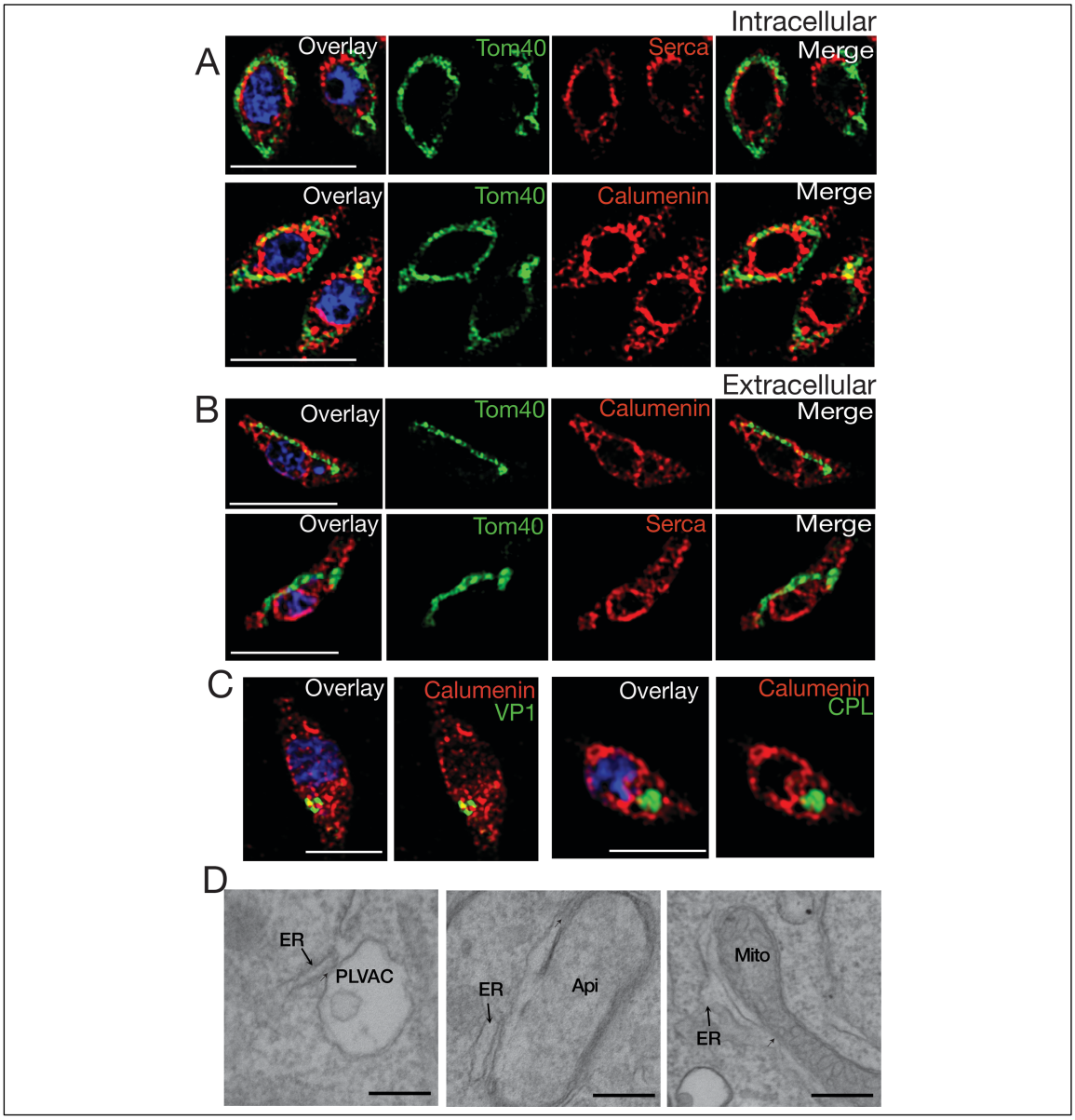

Figure 6: ER membrane contacts with the mitochondrion and the plant like vacuolar compartment (PLVAC). **A**, Super-resolution IFAs of intracellular parasites with the mitochondrion labeled with the αTom40 (green, 1:20,000) antibody and the ER labeled with the αTgcalumenin antibody (an ER calcium binding protein) (red, 1:1000) or the TgSERCA (red 1:1000). **B**, Immunofluorescence (IFA) of extracellular tachyzoites with the same antibodies used for part A. The mitochondrion and ER membranes interact in several regions. **C**, The PLVAC was localized with the αVP1 antibody (green, 1:200) or the αTgCPL antibody (green, 1:500). The ER membranes were labeled with the αTgERC antibody (red). The spots of contact between the ER and the PLVAC are yellow. Scale bars in A-C represent 5 μm. **D**, Transmission Electron Microscopy imaging of the contact sites formed between ER and PLVAC, ER and Apicoplast, ER and mitochondrial. Size bars are 100 nm.

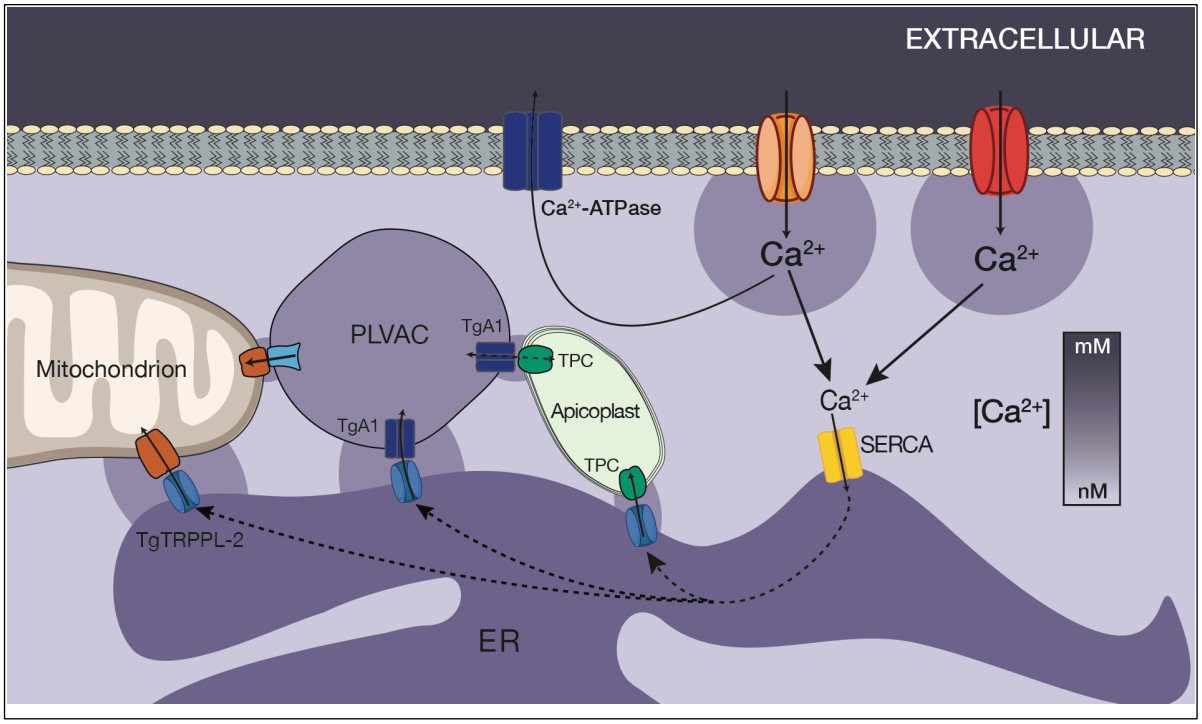

Figure 7: Model showing calcium entry through two different types of Ca^{2+} channels, uptake to the ER by SERCA and distribution to the other organelles via transfer from the ER to the mitochondria, PLVAC and apicoplast. In intracellular parasites, the mitochondria is in close contact with the ER which is constitutively leaking Ca^{2+} into the cytosol. The mitochondria take up Calcium from the ER through an unknown mechanism. VDAC could be involved in the transfer through the outer mitochondrial membrane (Mallo *et al.*, 2021). The PLVAC interacts with the ER and may also interact with the mitochondrion and the apicoplast. TgA1, a calcium ATPase previously characterized may be the pump involved in uptake (Luo *et al.*, 2001; Luo *et al.*, 2005). The mechanism of release is unknown. The TPC was shown to be involved in the formation of contacts between the ER and the apicoplast (Li *et al.*, 2021). Ca^{2+} could leak from the ER through the TgTRPPL-2 channel previously described (Marquez-Nogueras *et al.*, 2021).